Theses and Dissertations   Student Graduate Works

3-2002

Estimation of Atmospheric Precipitable Water Using the Global Positioning System

David A. Garay

Follow this and additional works at: https://scholar.afit.edu/etd

 Part of the Meteorology Commons

ESTIMATION OF ATMOSPHERIC PRECIPITABLE WATER
USING THE GLOBAL POSITIONING SYSTEM

THESIS

David A. Garay, 2nd Lieutenant, USAF
AFIT/GE/ENG/02M-07

DEPARTMENT OF THE AIR FORCE
AIR UNIVERSITY

AIR FORCE INSTITUTE OF TECHNOLOGY

Wright-Patterson Air Force Base, Ohio

Report Documentation Page

Report Date	Report Type	Dates Covered (from... to)
15 Mar 02	Final	Aug 2000 - Mar 2002

Title and Subtitle Estimation of Atmospheric Precipitable Water Using the Global Positioning System	**Contract Number**
	Grant Number
	Program Element Number
Author(s) 2Lt David A. Garay, USAF	**Project Number**
	Task Number
	Work Unit Number
Performing Organization Name(s) and Address(es) Air Force Institute of Technology Graduate School of Engineering and Management (AFIT/EN) 2950 P Street, Bldg 640 WPAFB, OH 45433-7765	**Performing Organization Report Number** AFIT/GE/ENG/02M-07
Sponsoring/Monitoring Agency Name(s) and Address(es) Air Force Weather Agency (AFWA) Technical Transition Team ATTN: Captain Robert T. Swenson, Jr. 106 Peacekeeper Drive, Suite 2N3 Offutt AFB, NE 68113-4039	**Sponsor/Monitor's Acronym(s)**
	Sponsor/Monitor's Report Number(s)
Distribution/Availability Statement Approved for public release, distribution unlimited	
Supplementary Notes The original document contains color images.	

Abstract

This research focuses on using the Global Positioning System (GPS) for atmospheric precipitable water (PW) estimation. Water vapor, measured in terms of PW, plays a crucial role in atmospheric processes and short-term weather forecasting. Traditional methodologies for measuring atmospheric water vapor distributions have known inadequacies, resulting in the motivation to gain good water vapor characterization via GPS. The ability to accurately forecast cloud formation and other weather phenomenon is critical, especially in the case of military operations. Using a network of GPS receivers, it is possible to estimate precipitable water throughout the network region with better accuracy than traditional methods and on a more consistent near real-time basis. First, an investigation into the effects of introducing less accurate, near real-time GPS ephemerides was accomplished. Secondly, the network geometry and data availability were degraded to simulate potential military operational constraints. Finally, several interpolation methods were applied to quantify the ability to estimate the water vapor distribution over the entire network region with limited data availability and network geometry constraints. Results showed that International GPS Service (IGS) ultra-rapid orbits introduced minimal PW estimation error (~1-2mm) while maintaining near real-time capability. The degraded perimeter network also introduced minimal PW estimation error (~1-2 mm) at the included stations, indicating potential application in constrained data environments. However, the interpolation investigation showed an overall inability to determine PW distribution over the entire network region.

Subject Terms

Global Positioning System, GPS, Differential Global Positioning System, DGPS, GPS Meteorology, GPS-MET, Precipitable Water, Atmospheric Water Vapor

Report Classification	Classification of this page
unclassified	unclassified

Classification of Abstract	Limitation of Abstract
unclassified	UU

Number of Pages

119

AFIT/GE/ENG/02M-07

ESTIMATION OF ATMOSPHERIC PRECIPITABLE WATER
USING THE GLOBAL POSITIONING SYSTEM

THESIS

Presented to the Faculty

Department of Electrical and Computer Engineering

Graduate School of Engineering and Management

Air Force Institute of Technology

Air University

Air Education and Training Command

In Partial Fulfillment of the Requirements for the

Degree of Master of Science in Electrical Engineering

David A. Garay, B.S.E.E.

2nd Lieutenant, USAF

March 2002

ESTIMATION OF ATMOSPHERIC PRECIPITABLE WATER
USING THE GLOBAL POSITIONING SYSTEM

David A. Garay, B.S.E.E.
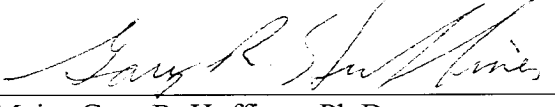2nd Lieutenant, USAF

Approved:

_____   *14 MAR 02*
Major John F. Raquet, Ph.D.
Assistant Professor, Committee Chairman

_____   *14 MAR 02*
Lieutenant Colonel Mike M. Miller, Ph.D.
Assistant Professor, Committee Member

_____   *14 Mar 02*
Major Gary R. Huffines, Ph.D.
Assistant Professor, Committee Member

Acknowledgments

I would first like to thank my thesis advisor Major John Raquet for the vast amount of support throughout this thesis research. His unparalleled teaching ability and substantial GPS technical expertise proved to be critical assets in successful completion. Moreover, his officer mentorship, spiritual leadership, and faithful support proved to be invaluable resources in both my personal and professional development at AFIT. The TDY to Switzerland was truly great! Thank you for all of your contributions and efforts.

Without further delay, a huge thanks to all my colleagues and friends. You are all the best group of people I have ever had the honor to serve (and study) with. 2Lt Greg Hoffman, thanks for your regular support and loyal friendship. You, the notorious G.R.E.G., are like a brother and always were there to help drag me through the AFIT jungle. Capt Mike "Nugget" Giebner, thanks for your undying friendship and the opportunity to learn from your many experiences over the past half century. You have truly educated me in the "finer" things this life has to offer. FltLt Matt Papaphotis, thanks for teaching me how to have a true free spirit. You make a pretty good honorary Australian-Wisconsinite! Furthermore, a special thanks to all my classmates in the guidance, control, and navigation section for the good humor and undying sarcasm to help us get through those long AFIT days.

Lastly, I would like to thank my wife for all the undying support and love that made this successful research possible. You have given me exceeding amounts of encouragement and admiration; more than I have ever thought possible. And finally, thank you LORD for seeing me through and blessing me beyond all imagination.

Table of Contents

List of Figures

List of Tables

Abstract

This thesis focuses on using the Global Positioning System (GPS) for atmospheric precipitable water (PW) estimation. Water vapor, measured in terms of PW, plays a crucial role in atmospheric processes and short-term weather forecasting. Traditional methodologies for measuring atmospheric water vapor distributions have known inadequacies, resulting in the motivation to gain good water vapor characterization via GPS. The ability to accurately forecast cloud formation and other weather phenomenon is critical, especially in the case of military operations.

Using a network of GPS receivers, it is possible to estimate precipitable water throughout the network region with better accuracy than traditional methods and on a more consistent near real-time basis. First, an investigation into the effects of introducing less accurate, near real-time GPS ephemerides was accomplished. Secondly, the network geometry and data availability were degraded to simulate potential military operational constraints. Finally, several interpolation methods were applied to quantify the ability to estimate the water vapor distribution over the entire network region with limited data availability and network geometry constraints.

Results showed that International GPS Service (IGS) ultra-rapid orbits introduced minimal PW estimation error (~1-2 mm) while maintaining near real-time capability. The degraded perimeter network also introduced minimal PW estimation error (~1-2 mm) at the included stations, indicating potential application in constrained data environments. However, the interpolation investigation showed an overall inability to determine PW distribution over the entire network region.

ESTIMATION OF ATMOSPHERIC PRECIPITABLE WATER

USING THE GLOBAL POSITIONING SYSTEM

I. Introduction

1.1 Background

Accurate and reliable short-term weather forecasting has consistently been a shortcoming in the meteorological community. Everyone is affected by short-term weather in one way or another. Whether it is a farmer trying to maintain his crops or a family trying to get together for a picnic, plans can be impacted by the daily weather patterns. The military is particularly concerned with the weather while military operations are being executed. Missions of all scales, from bombing missions to fighter sorties, are significantly impacted by the daily weather and need to take possible weather development into consideration.

During the Gulf War, the weather was fairly predictable as operations took place over the arid region of the Middle East. This arid region, along with other arid areas worldwide, offers an atmosphere where weather is not as variable as it is in other regions. Hot sunny days, cool brisk nights, and the absence of cloud cover were the normal conditions. As a result, the weather was a relatively subtle factor to consider except when a significant, impacting change took place (i.e., a sandstorm). However, in operations over Bosnia, a very different situation, where weather was possibly the biggest factor in the planning and execution of aerial missions. Here, in the rich European climate off the coasts of the Mediterranean Sea, weather is much more variable as there is

substantially more moisture content in the atmosphere. This leads to periods of persistent cloud cover, combined with the daily concern of stormy and fast moving severe weather, which could drastically impact the operations over the region.

Water vapor is a significant component of the Earth's atmosphere, and its interaction with other atmospheric constituents correlates strongly with daily weather patterns. Precipitable water (PW) is the amount of water (usually measured in millimeters) that would result from taking a cylindrical column of air from the earth's surface to the top of the atmosphere, and condensing all of the water vapor in that column. Traditional methodologies have been employed in the estimation of precipitable water for more than half a century. However, the inadequacies and shortcomings of these traditional methods have prevented the gathered data from significantly contributing to accurate weather forecasting.

With the recent implementation of the Global Positioning System (GPS), a new method for precipitable water determination has come about. The continuously broadcast GPS signals are refracted and delayed as they propagate through the Earth's atmosphere. The physics and properties of electromagnetics allow us to utilize these refracted signals to mathematically calculate the amount of precipitable water in the atmosphere over a given location. Calculation of precipitable water via GPS has several advantages to include better precision, real-time capability, cost effectiveness, and global availability. With these improvements, gathering more numerous and more accurate data about the water vapor fields over a geographic region has become a realistic possibility. In turn, meteorologists can utilize this improved information to expand their understanding of the role precipitable water plays in the atmosphere resulting in better prediction of short-term

weather patterns, and allowing for the enhancement of weather-dependent planning efforts.

1.2 Problem Definition

The initial goal of this thesis is to calculate the precipitable water over the locations of specific GPS receivers. Then, the utilization of interpolation methods will allow for the determination of water vapor distribution over the investigated region covered by a network of GPS receivers. This work has already been accomplished in the civilian sector, and the objective is to recreate these efforts as accurately as possible. This initial goal of process recreation will establish the basis for further investigation.

The primary goal, which also serves as the purpose for this thesis, is to evaluate the practical military considerations for utilizing a GPS-based method in determining PW. This will require implementing regular civilian assumptions and testing them against practical military operational concerns. The hostile operating environment must be considered, as it poses several obstacles and limitations that are not present in the civilian meteorology community.

To accomplish these goals, it is important to first get a thorough understanding of what the civilian GPS meteorology research has accomplished, as there has been no military involvement in the research to date. Once the military community is educated on the theory and methodologies for GPS precipitable water determination, that knowledge can be utilized to examine the more specific aspects required due to the additional restrictions imposed by operating in a combat environment.

1.3 Summary of Current Knowledge

With hundreds of continuously operating GPS reference receivers located throughout the world, the network they comprise presents a valuable resource of information. One example is the United States' Continuously Operating Reference Station (CORS) network maintained by the National Oceanic and Atmospheric Administration's (NOAA) office of the National Geodetic Survey (NGS). The CORS network is composed of GPS reference stations throughout the U.S. and its territories, composing a significant portion of the total reference stations located around the globe [8]. CORS and other similar interrelated networks can provide continuous, real-time data that could be used to calculate weather data. Additionally, the vast network would make it possible to gather precipitable water information nearly anywhere on the globe where GPS is being utilized. Ideally, this data stream could compliment existing precipitable water data collection sources, resulting in increased water vapor distribution knowledge, and enabling more accurate forecasts of rainfall and severe weather [2]. Furthermore, the satellite signal characteristics and the precipitable water algorithm lead to a solution absent of the many errors associated with traditional determination methods. This allows for comparable, if not superior, accuracies in precipitable water estimation via GPS.

Most geodetic GPS algorithms are primarily concerned with relative positioning, but they also determine the delay or extra electromagnetic wave path length of the introduced by the earth's atmospheric refractivity [3]. Precipitable water calculations utilize the delay or extra path length caused by the neutral atmosphere, called the troposphere. In this region, there are essentially two components to the induced delay: a hydrostatic (dry) delay and a wet delay term. Both of the delays are generally the

smallest for paths oriented in the zenith direction (90° elevation), and increase as the satellite elevation angle decreases. A mapping function is utilized to convert a delay term to its equivalent zenith delay. A simple mapping function for the hydrostatic and wet delays is $(\sin e)^{-1}$, where e is the corresponding satellite elevation [3].

The tropospheric dry delay term can be easily determined from pressure and temperature measurements at the Earth's surface. However, the atmospheric water vapor is distributed much more unevenly, leading to the inability to utilize the same surface parameters to completely determine the wet delay. This is the motivation for an enhanced GPS technique for water vapor determination, as wet delay is directly related to the quantity of water vapor overlying the receiver [3]. The quantity of precipitable water is directly related to the zenith wet delay (ZWD), which is the satellite signal wet delay mapped to the zenith direction. A multiplicative constant Π is the conversion factor, and its primary parameters are known atmospheric physical property constants. These atmospheric constants include the density of liquid water, specific gas constant for water vapor, and atmospheric refractivity constants. The value of Π is not a universal constant, but rather one that changes with both location and atmospheric conditions. It is calculated given a specific location and atmospheric surface measurements, and its accuracy is simply limited by the accuracy and to determine these parameters.

1.4 Assumptions

This thesis research is primarily dependent upon processing the GPS signal data gathered at specific locations. In light of this data dependence, several issues must be taken into consideration. First, the data for the CORS network will continue to be

archived and accessible on the Internet. Future research applications would need to assume that the GPS network would continue to operate as it does at present.

Secondly, it is assumed that the GPS processing software can effectively process the data, producing accurate results. This would include the premise that the chosen software package synthesizes the data using methodologies comparable to other similar GPS processing software. This is crucial when comparing data from different sources that use different software packages.

Furthermore, it is assumed that consistent and accurate GPS network station coordinates are being employed. This is critical due to the magnitude of the tropospheric delay term under investigation, as small errors in the coordinates will multiply their effect in the tropospheric delay. Finally, it is assumed that the network and orbit degradation investigations will not result in the processing software becoming incapable of resolving all the ambiguities needed to produce viable tropospheric delay data.

1.5 Scope

This research utilizes previous GPS data that has been recorded and determines the precipitable water at a given location and region for a particular timeframe. Although the real-time application possibility does exist, it will not be implemented in this study and will be left as a possible application for future research and investigation. This is primarily due to the additional complexities associated with real-time implementation and the associated hardware. Moreover, the time and resources for such an endeavor are limited, restricting the magnitude of the study.

Military applications will also be evaluated, particularly investigating the additional restrictions and limitations imposed by military operating conditions. However, this study will not use actual data from military systems for implementation purposes. Data compatibility issues will be investigated and sample data may be utilized to determine the feasibility of integrating this type of system. Also, simulated network environments will be examined to evaluate the military concerns. In this study there will be no real-world implementation of a receiver network in a hostile foreign environment. However, the various factors that must be considered when deploying such a system will be evaluated.

Most importantly, this study emphasizes the mechanics of estimating the parameter of precipitable water from the engineering perspective. There will be no interpretation of the results in the terms of weather forecasting. The accuracy of determining the actual precipitable water value is this research's focal point.

1.6 Standards

NOAA has established a subset of the CORS network for the purposes of calculating precipitable water. These GPS-meteorology (GPS-MET) network stations have been equipped with surface meteorology instruments to measure all the parameters necessary to calculate precipitable water via GPS, such as surface pressure and temperature. The satellite observation files, meteorological measurement files, and the NOAA calculated precipitable water values all are archived and accessible via the Internet [10]. To provide initial validation to the methodology employed in this thesis, a comparison will be made between the NOAA-calculated and the thesis-calculated

precipitable water values. This will be the primary standard for determining if the thesis methodologies are implemented properly and producing comparable results.

Additionally, the statistics for GPS-derived precipitable water values will be compared to other traditional meteorological estimation methods. In particular, it is important to make a comparison in the relative errors encountered in this study versus the regularly experienced error fluctuations experienced by traditional estimation methods. This comparison makes it possible to get a feel for not only how accurate the GPS-based method is, but also how significant the variations in the relative error are.

1.7 Methodology

The first step in accomplishing this thesis was to gather all the background information necessary to more completely understand the problem being addressed. A literature review was conducted to evaluate the need for an additional precipitable water calculation method, the current methods of doing so, and what contributions this thesis could make to the civilian efforts already underway.

After problem formulation, the proper software for analyzing the GPS data was sought out and chosen. The Bernese GPS Software was chosen as the best software package to accomplish the analysis required for this thesis. This software is a GPS analysis tool meeting the highest quality standards for geodetic applications using the GPS, and is used worldwide for high-precision implementations [5]. The versatility and effectiveness of the Bernese software, along with the readily available product support, made it a clear choice for our implementation. After proper familiarization with the Bernese software, sample data from an arbitrary initial receiver network was chosen to

run through the software, gaining initial insight into what kind of GPS receiver network would be best for the focus of this thesis. Additionally, working with this initial trial network provided the necessary experience for refining and solidifying of the analysis processes to be used.

The next significant step was to choose the network for focused examination. Geographic location, network geometry, receiver density, weather activity, and availability were all weighted factors in choosing the appropriate GPS receiver network. Once the network had been determined, actual precipitable water calculation over the associated region began, utilizing the Bernese GPS software and MATLAB$^{\circledR}$. For primary validation, the results were compared with NOAA GPS precipitable water calculations. Additionally, the relative errors of the GPS precipitable water determination were related to the typical errors seen in traditional determination methods.

After substantially "good" results had been obtained, investigation into additional military implementation issues began. Network and orbit degradations were investigated and were initially the most important issue to resolve. This degradation investigation provided key insight into the feasibility of utilizing GPS precipitable water determination methods for military applications. Both the orbit and network degradations were examined over the GPS station networks as defined previously. Once the degradation effects on precipitable water resolution were evaluated, the second issue of interpolation of the precipitable water over the degenerated network was examined. This interpolation examination proved pivotal in drawing conclusions about the military implementation issues.

1.8 Thesis Overview

Chapter 2 touches upon the current, traditional precipitable water determination methods in more detail. The chapter continues by focusing on the GPS theory, which serves the basis for the mathematical model of the precipitable water algorithm. The GPS signal characteristics and transmission through the atmosphere are the focus of this discussion, as they are fundamental to the determination of precipitable water. Chapter 2 also describes the mathematical algorithms for calculating precipitable water using these investigated transmitted signal properties.

Chapter 3 describes the methodology this thesis took in experimenting with the precipitable water determination process. This primarily includes determining and describing the previously developed algorithm's flow. Additionally, the experimentation process used to evaluate the effectiveness of determining precipitable water via GPS is described. Chapter 4 displays and quantifies the results obtained through this experimentation process, and strives to present substantial evidence to support our conclusions and inferences in Chapter 5.

Chapter 5 summarizes the entire thesis effort, and focuses on the major experimental findings. Moreover, this chapter aims to answer the questions posed in the problem statement based on the results seen in Chapter 4. Chapter 5 also poses questions and additional research considerations, based on the findings in this research.

II. Theory

2.1 Overview

This chapter describes the traditional precipitable water determination methods and their performance characteristics in detail. Other topics include underlying GPS principles, the physical properties that directly effect the GPS precipitable water calculations, and the mathematical algorithms required for GPS determination of precipitable water.

2.2 Traditional Precipitable Water Determination

Precipitable water is an atmospheric element that plays a critical role in atmospheric processes on all scales. The activity of precipitable water in the atmosphere affects everything from micrometeorology to global climate [1]. Of all atmospheric constituents, precipitable water is the most variable, and it is directly related to the formation of clouds and storms [1]. Atmospheric scientists have traditionally used two principal methods for the measurement of the vertical and horizontal distribution of water vapor – radiosondes and water vapor radiometers. These devices will be described in the following sections.

2.2.1 Radiosondes

The primary traditional technique is a simple balloon-launched sensor system known as a radiosonde. These devices are considered expendable, costing an average of

$250 per release. The National Meteorological Center and similar weather forecast centers use radiosondes as the cornerstone for their operational analysis, but the sheer cost of the instruments limits their release to twice daily at a limited number of weather observation stations [12]. These restrictions pose several problems regarding the adequate resolution of atmospheric water vapor distributions. First, it is apparent that real-time or near real-time data acquisition is impossible. This poses a significant shortcoming, as water vapor variations occur on a much finer scale than those associated with temperature or winds [1]. Therefore, the data acquired at these instances is only good for the short time immediately following its collection.

A second significant flaw involves the flight path of the radiosonde. Ideally, forecasters would desire a straight vertical (zenith) flight path, as the precipitable water over a given location depends only on the atmosphere directly overhead. However, a ballooned instrument like a radiosonde is highly susceptible to drifting off at the whim of the atmospheric currents and conditions, seldom maintaining its desired flight path. Additional complications are caused by the need to man the of the radiosonde surface launch station during its flight through the atmosphere. This flight trajectory can range from minutes to an hour; all depending on how fast the atmospheric conditions permit the ballooned instrument to ascend to its full altitude. The flight time aspect also makes it impossible to achieve the desired real-time capability.

2.2.2 Water Vapor Radiometer (WVR)

The second traditional method for atmospheric precipitable water determination is a water vapor radiometer (WVR). Two water vapor radiometer types are used: ground-

based and satellite-based. Ground-based, upward-looking water vapor radiometers scan the sky, measuring the microwave radiation that is emitted by the water vapor in the atmosphere against the cold background of space. This is possible due to the frequency dependence of the sky brightness temperature [12]. However, these ground-based water vapor radiometers do have a variety of inadequacies. First, ground-based WVRs are severely affected under heavy cloud cover and adverse weather conditions. In fact, most of these devices provide no useful data when it is raining [12]. Furthermore, they are not very mobile as they are somewhat bulky, must be calibrated for a specific location, and are also quite expensive ($100k's each). Therefore, these devices are most commonly employed at a single location for a specific application.

Satellite-based, downward-looking WVRs work on the same principal; however, they utilize the hot background provided by the earth as a reference.   Space-based WVRs have similar, but more limiting drawbacks in comparison to the ground-based WVRs. Due to extensive land surface temperature variability, their usefulness is usually restricted to operation over ocean regions. Obviously, this is a very limiting restriction, as forecasting interests lie primarily over the continental land regions where much of the weather patterns effecting daily operations take place. Also, their performance is significantly reduced during light to moderate cloud cover, considerably limiting their usefulness [12]. Moreover, although satellite-based WVRs provide good spatial coverage, they are constantly in motion and provide inconsistent coverage over a given location. On the whole, the price and complications associated with both ground-based and satellite-based water vapor radiometers make consistent widespread real-time application nearly unachievable.

2.2.3 Traditional Precipitable Water Characterization

The shortcomings associated with both traditional methods have left precipitable water as one of the most poorly characterized meteorological parameters. Meteorologists and scientists alike agree that water vapor fields are inadequately defined on all levels of weather analysis and forecasting [13]. As discussed previously, this inadequacy stems from the sporadic nature of precipitable water observations and the highly variable nature of water vapor in the atmosphere. Moreover, because of its high variability and poor characterization, precipitable water is recognized as the primary error contributor in short-term (i.e., daily and hourly) weather forecasts. It is widely appreciated within the weather community that improved atmospheric precipitable water monitoring will lead to improved precipitation forecasting, and better tracking of severe weather progression [4].

2.3 Precipitable Water Determination Using GPS

With continuously operating GPS receivers existing in large numbers, the existing GPS networks could provide an important data stream for meteorological purposes [2]. These networks are capable of generating the real-time data. Additionally, the vast network would make it possible to gather water vapor information nearly anywhere on the globe where GPS is being utilized. Moreover, the precipitable water calculation via GPS merely involves processing existing GPS data files, with no additional hardware or equipment requirements. Ideally, this data stream could complement existing water vapor data collection sources, resulting in improved water vapor distribution knowledge and enabling more accurate forecasts of rainfall and severe weather [2]. Furthermore, the

satellite signal characteristics and the precipitable water algorithm lead to a solution not containing the many errors associated with traditional precipitable water determination methods. This allows for comparable, if not superior, accuracies in estimating precipitable water via GPS.

2.3.1 GPS Satellite Ephemerides

In order to process GPS satellite observation data, corresponding satellite ephemeris data must also be utilized. This ephemeris data provides the information needed to calculate each GPS satellite's earth-centered earth-fixed (ECEF) position at any arbitrary time (within the validity window). Several types of ephemerides exist with varying accuracy and availability. Table 2-1 displays the key characteristics for each of the four standard ephemeris types.

Table 2-1. Comparison of Satellite Ephemeris Types [6]

GPS Satellite Ephemeris	Accuracy	Latency
Broadcast	~260 cm / ~7 ns	real-time
Ultra-Rapid (Predicted)	~25 cm / ~5 ns	real-time
Rapid	5 cm / 0.2 ns	17 hours
Precise (Final)	<5 cm / 0.1 ns	~13 days

Broadcast ephemerides are the most easily accessible, as they are transmitted continuously and are normally archived with the satellite observation files for a particular station. These ephemerides are a predicted orbit, calculated from satellite observations recorded at five globally located permanent reference stations. A predicted orbit takes all the satellite observations leading up to a certain time, and predicts where the satellite will be based upon these observations. Unfortunately, broadcast ephemerides have the lowest

accuracy of those considered, significantly degrading precipitable water estimation accuracy. The small number of permanent reference stations and the once per day calculations are the primary contributors to the broadcast ephemeris imprecision [11]. This attribute makes broadcast ephemerides unsuitable for high accuracy analysis of precipitable water, but given their high accessibility and real-time availability, they may be useful for coarse analysis. Moreover, the GPS operational control segment, independent from existing civilian GPS networks, generates broadcast ephemerides [11].

Ultra-rapid orbits present another real-time possibility at the expense of some accessibility. Produced by the International GPS Service (IGS), ultra-rapid orbits are also a predicted orbit product. However, they are an order of magnitude better in accuracy when compared to the broadcast ephemerides. The IGS utilizes the Internet to get satellite observation data from about 40 of its permanent reference stations, with the increase in the number of incorporated reference stations resulting in an increase in accuracy. The IGS generates two ultra-rapid orbit ephemerides per day with an average delay of 9 hours [5]. However, it would be possible to calculate a similar predicted orbit on a near real-time basis with access to the observation data and capable processing software. NOAA's GPS-MET network utilizes the Scripps Orbit, a Scripps Institute predicted orbit product, in conjunction with their GPS at MIT (GAMIT) processing software. The Scripps Orbit is of equivalent accuracy to the IGS ultra-rapid predicted orbit, but is produced with only a 1-2 hour delay and is formatted for use with the GAMIT software [10].

To achieve further ephemeris accuracy improvements, posteriori satellite observation information is required in addition to the a priori information utilized in a

predicted orbit. The IGS rapid orbit product utilizes additional satellite observations after the time of interest to make a more accurate determination of where the satellite actually was at that time. Approximately 17 hours of additional a posteriori satellite observations are used to better estimate the satellite position and velocity at the time of interest. Rapid orbits present significant accuracy improvements over the predicted orbit products, but have about a 24-hour delay in their availability due to the incorporation of a posteriori data [5].

The highest accuracy can be achieved using more a posteriori satellite observation data. The IGS produces a final or precise orbit product utilizing approximately 13 days of additional a posteriori data from its reference station network. The additional data enables a more accurate satellite ephemeris determination, which removes most of the error present in less accurate ephemerides. The precise ephemeris is preferred when working with high accuracy GPS applications, as the error introduced by the precise ephemeris is almost insignificant when compared to other error sources. However, the nature of producing a precise orbit introduces about a 2-week delay in availability [5]. Therefore, the most accurate data processing possible cannot begin until two weeks after the time of interest, so it is not useful for systems requiring real-time processing.

2.3.2 Atmospheric Refraction of GPS Signals

Geodetic GPS algorithms have the secondary result of calculating the delay or extra path length associated with the electromagnetic waves, which is introduced by means of the atmosphere's refractivity [3]. These delays are essentially errors that must

be removed for precise position determination. The Earth's atmospheric layers, from the GPS community's perspective, can be seen in Figure 2-1.

```
+--------------------------------------+
|                                      |
|              Ionosphere              |
|          (Charged Atmosphere)        |
|                                      |
|                                      |
| ~50 kilometers                       |
+--------------------------------------+
|                                      |
|              Troposphere             |
|          (Neutral Atmosphere)        |
|                                      |
|                                      |
| 0 kilometers                         |
+--------------------------------------+
```
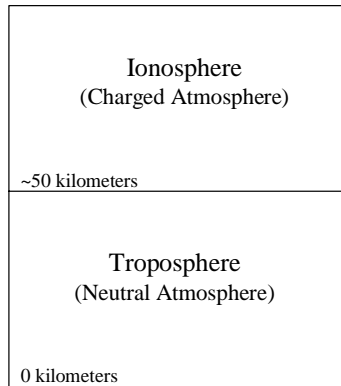
Figure 2-1. Earth's Atmospheric Layers Relevant to GPS Signal Propagation

The original GPS developers never intended, or perhaps even imagined, these introduced delays would be utilized for further analysis and examination. The original intent was to effectively eliminate the delay, thereby gaining the best possible positioning accuracy. However, advanced GPS studies have resulted in numerous non-positioning applications to include precipitable water estimation.

The atmospheric layers shown in Figure 2-1 represent the two atmospheric components affecting GPS measurements: the ionosphere and troposphere. The ionosphere consists of free ions found in the upper atmosphere – typically above 50 kilometers. The ionosphere is an atmospheric region that introduces a delay to the satellite signal that can be eliminated by using dual frequency measurements. The remainder of the atmospheric delay can be attributed to the electrically neutral portion of the atmosphere, known as the troposphere – typically from the surface up to about 50 kilometers. This tropospheric region is essentially where all the Earth's weather activity takes place, and thus is the region of interest for this study in precipitable water

determination. In this region, there are two components to the induced delay: a hydrostatic (dry) delay and a wet delay term. Both delays are generally the smallest for satellites oriented in the zenith direction and increase as the satellite elevation angle decreases. This makes sense because GPS signals at lower elevation angles travel through more of the Earth's atmosphere, producing a longer delay. This concept is illustrated in Figure 2-2.

Zenith Satellite

Lower Elevation Satellite

Neutral Atmosphere
Boundary

*Note: not to scale

Ground   Antenna
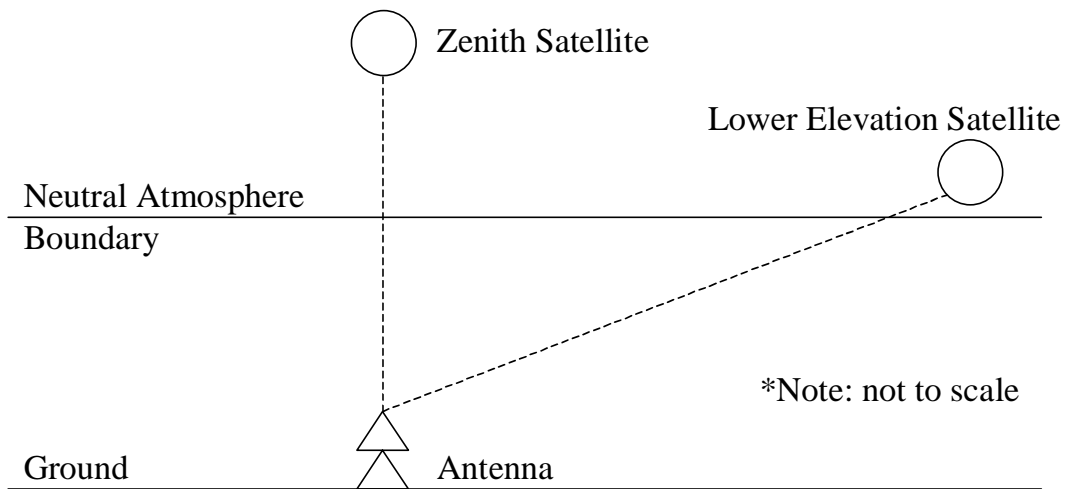
Figure 2-2. Satellite Elevation Illustration [9]

Lower satellite elevations create observations that are much more corrupted by tropospheric refraction and multipath than those at high elevations. Setting a lower bound or satellite elevation mask of 10 or 15 degrees can remove the noisiest observations for traditional geodetic purposes [5]. However, through the use of these lower elevation observations, it may be possible to improve the estimated zenith tropospheric delay accuracy. This is due to the increased atmospheric information contained within these lower elevation observations as the signal travels through larger sections of the Earth's atmosphere. Proper weighting of these corrupted lower elevation

observations and use of accurate tropospheric mapping functions can result in increased

ability to estimate zenith tropospheric delay [5].

2.3.3   Tropospheric Mapping Functions

A mapping function is utilized to convert an elevation-specific delay term to its

equivalent zenith delay. A rough mapping function for both the hydrostatic and wet

delays is the inverse of the sine of the satellite elevation [3]. This inverse sine mapping is

also known as the "cosecant law" and assumes both constant atmospheric refractivity and

a flat earth surface [14]. Equation 2-1 shows the conversion from wet delay (WD) to

zenith wet delay (ZWD) for a satellite elevation e using the "cosecant law."

$$ZWD = (\sin e)^{-1} * WD \tag{2-1}$$

More accurate mapping functions utilize further advanced algorithms to map the

tropospheric delay to the zenith direction. For example, the Saastamonien and Baby, et.

al. mapping functions basically extend the "cosecant law" to provide improved accuracy

[14]. Other, more complex mapping functions are based on the truncation of a continued

fraction representation, as shown in Equation 2-2 [14].

$$m(\varepsilon) = \cfrac{1}{\sin\varepsilon + \cfrac{a}{\sin\varepsilon + \cfrac{b}{\sin\varepsilon + \cfrac{c}{\sin\varepsilon + \dots}}}} \tag{2-2}$$

The Marini mapping function forms the basis for many of these continued fraction

mapping methods, essentially showing that the tropospheric delay mapping function $m(\varepsilon)$

can be expressed as a continued fraction combination using the corresponding satellite

elevation angle ε. In the Marini continued fraction expression, the coefficients a, b, c …

are constants or linear functions [14].

The Neil mapping function also utilizes the continued fraction expression, with

slightly different representations for the hydrostatic and wet delay components.

Combining the mapped hydrostatic and wet delays results in the equivalent total

tropospheric delay, illustrated in Equation 2-3 [14]

$$d_{Trop} = d_{Hydro}^{Z} m_{Hydro}(\varepsilon) + d_{Wet}^{Z} m_{Wet}(\varepsilon) \tag{2-3}$$

where
$$d_{Hydro}^{Z} = \text{zenith hydrostatic delay}$$
$$d_{Wet}^{Z} = \text{zenith wet delay}$$
$$m_{Hydro}(\varepsilon) = \text{hydrostatic mapping function}$$
$$m_{Wet}(\varepsilon) = \text{wet mapping function}$$
$$\varepsilon = \text{satellite elevation}$$

The combined use of both mapping functions reduces errors in geodetic estimation for

observations as low as 3° in elevation, and agrees as well or better than mapping

functions calculated from radiosonde profiles. The Neil mapping function variability is

best modeled by latitude and seasonal dependence, and is attributed to the variation of

solar radiation. To account for the decreasing atmospheric "thickness" as the station

height increases, the height above the geoid is account for in the hydrostatic mapping

component [14]. The Neil hydrostatic mapping function is shown in Equation 2-4.

$$m_{Hydro}(\varepsilon) = \frac{\dfrac{1}{1+\dfrac{a_{hydro}}{1+\dfrac{b_{hydro}}{1+c_{hydro}}}}}{\sin\varepsilon + \dfrac{a_{hydro}}{\sin\varepsilon + \dfrac{b_{hydro}}{\sin\varepsilon + c_{hydro}}}} + \left[\frac{1}{\sin\varepsilon} - \frac{\dfrac{1}{1+\dfrac{a_{ht}}{1+\dfrac{b_{ht}}{1+c_{ht}}}}}{\sin\varepsilon + \dfrac{a_{ht}}{\sin\varepsilon + \dfrac{b_{ht}}{\sin\varepsilon + c_{ht}}}} \right] \times \frac{H}{1000} \tag{2-4}$$

The coefficients a_{ht}, b_{ht}, and c_{ht} are constants, whereas a_{hydro}, b_{hydro}, and c_{hydro} are interpolated based on average values for known latitudes [14]. The Neil wet mapping function is shown in Equation 2-5.

$$m_{Wet}(\varepsilon) = \frac{\dfrac{1}{1+\dfrac{a_{wet}}{1+\dfrac{b_{wet}}{1+c_{wet}}}}}{\dfrac{1}{\sin\varepsilon+\dfrac{a_{wet}}{\sin\varepsilon+\dfrac{b_{wet}}{\sin\varepsilon+c_{wet}}}}}$$

(2-5)

Again, the coefficients a_{wet}, b_{wet}, and c_{wet} are interpolated based on average values for known latitudes [14].

2.3.4 Removal of Hydrostatic Delay Component

The hydrostatic delay is attributed to the transient or induced dipole moment of all the gaseous constituents in the atmosphere, to include water vapor [3]. This dry delay term can easily be determined from surface pressure and temperature measurements, due to the relationship between the hydrostatic delay relative to the atmospheric elevation. The hydrostatic portion of the tropospheric delay can be calculated by means of Equation 2-6 [1]

$$ZHD = \frac{(2.2779 \pm 0.0024)P_s}{1 - 0.00266\cos 2\lambda - 0.00028H}$$

(2-6)

where
$\quad ZHD$ = zenith hydrostatic delay (millimeters)
$\quad P_s$ = the pressure at the Earth's surface (millibars)
$\quad \lambda$ = latitude of location
$\quad H$ = height of surface above ellipsoid (kilometers)

The hydrostatic delay calculation regularly achieves very precise results with accuracies on the order of 1 mm or less.

However, the atmospheric water vapor is much more unevenly distributed, so the same surface parameters cannot completely determine the wet delay. This uneven distribution motivates the GPS technique for precipitable water determination, as wet delay is directly related to the quantity of water vapor overlying the receiver [3]. The zenith wet delay can range from less than 10mm in arid regions to over 400mm in extremely humid regions. Additionally, the wet delay variability consistently exceeds that of the hydrostatic delay by more than an order of magnitude [3].

2.3.5 Mathematical Algorithm for Precipitable Water Determination

The zenith wet delay can be determined via GPS data utilizing the overall least-squares position solution, GPS satellite orbital parameters, and several other fundamental parameters. The theoretical definition states that if water vapor is integrated in terms of precipitable water (PW), the height of an equivalent column of liquid water is [3]

$$PW = \int_0^\infty r \frac{\rho_a}{\rho_w} dz \qquad (2\text{-}7)$$

where
$$\rho_a = \text{density of dry air}$$
$$\rho_w = \text{density of liquid water}$$

The variable r is known as the mixing ratio, and is calculated empirically by

$$r = \frac{\text{mass of water vapor}}{\text{mass of dry air}} \qquad (2\text{-}8)$$

Although this theoretical definition is valid, the mixing ratio r is never known at every location in the Earth's atmosphere. Recall that the tropospheric wet delay is directly related to the quantity of water vapor overlying the receiver [3]. Therefore, by

utilizing an indirect approach, the quantity of precipitable water can be related to the

zenith wet delay (ZWD) at the receiver location by [2]

$$PW = \Pi \times ZWD \qquad (2\text{-}9)$$

where the ZWD is given in units of length (typically meters) and Π is the dimensionless

constant of proportionality. The constant Π can be calculated by [2]

$$\Pi = \frac{10^6}{\rho_w R_v \left(\dfrac{k_3}{T_m} + k_2' \right)} \qquad (2\text{-}10)$$

where

$$\rho_w = \text{density of liquid water}$$
$$R_v = \text{specific gas constant for water vapor}$$

The constant k_2' is determined by

$$k_2' = k_2 - mk_1 \qquad (2\text{-}11)$$

The value of m is a ratio defined by

$$m = \frac{M_v}{M_d} \qquad (2\text{-}12)$$

where

$$M_v = \text{molar mass of water vapor}$$
$$M_d = \text{molar mass of dry air}$$

The physical constants k_1, k_2, and k_3 are taken from the widely used formula for

atmospheric refractivity N defined by

$$N = k_1 \frac{P_d}{T} + k_2 \frac{P_v}{T} + k_3 \frac{P_v}{T^2} \qquad (2\text{-}13)$$

2-14

where

$$P_d = \text{partial pressure of dry air}$$
$$P_v = \text{partial pressure of water vapor}$$
$$T = \text{absolute temperature}$$

Several studies have resolved values for the atmospheric refractivity constants k_1, k_2, and k_3. Direct refractivity constant measurements were taken using microwave techniques prior to the 1960's. Smith and Weintraub (1953) compiled and averaged the early microwave measurements, while Hasegawa and Stokesbury (1975) compiled and characterized many more experimental microwave results [2]. Thayer (1974) utilized another approach utilizing optical frequencies to determine the atmospheric refractivity constants values. The microwave study undertaken by Hasagawa and Stokesbury (1975) is the most comprehensive and accepted study, but the details of their statistical approach is not completely agreed upon [2]. As a result, Bevis et al. reanalyzed their compilation using a conservative estimation of the uncertainties and increased the emphasis on obtaining more robust results. This reanalysis produced values for the atmospheric refractivity constants used by most of the GPS meteorology community and are shown below [2].

$$k_1 = 77.60 \pm 0.05 \text{ K mb}^{-1}$$
$$k_2 = 70.4 \pm 2.2 \text{ K mb}^{-1}$$
$$k_3 = 3.739 \pm 0.012 \times 10^5 \text{ K}^2 \text{ mb}^{-1}$$

The theoretical definition of the parameter of T_m is a weighted mean atmospheric temperature defined by [1]

$$T_m = \frac{\int \frac{P_v}{T} dz}{\int \frac{P_v}{T^2} dz} \tag{2-14}$$

2-15

where

$$P_v = \text{partial pressure of water vapor}$$
$$T = \text{absolute temperature}$$

Again, this theoretical definition is impossible to implement, as the absolute temperature T is not known at every point in the Earth's atmosphere. As a result, location dependent regressions have been developed to closely approximate the mean temperature T_m value based on the surface temperature T_s. The standard regression utilized within the United States by atmospheric scientists and meteorologists alike is

$$T_m = 70.2 + 0.72T_s \qquad\qquad (2\text{-}15)$$

This regression was developed from an analysis of 8718 radiosonde profiles flown over a two-year period from sites within the United States. These sites had locations ranging from 27° to 65° in latitude and a height ranging from 0 to 1.6 kilometers.

2.3.6   Error and Variability Discussion

Roughly speaking, the ratio of PW/ZWD should equal the constant of proportionality Π, having the approximate value of 0.15. However, the actual value of Π depends upon local conditions such as location, elevation, season of year, and weather, having variability as much as 15% [3]. The variability of Π is derived nearly in its entirely from the variability of T_m and in the physical refractivity constants k_1, k_2, and k_3. Figure 2-3 shows the variance in the constant of proportionality, Π, in relation to the mean atmospheric temperature, T_m.
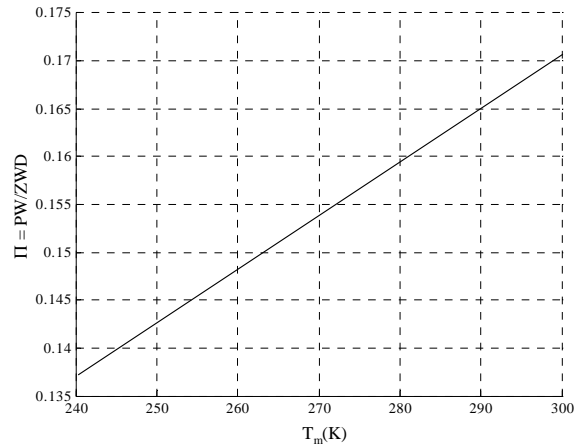
Figure 2-3. Variance of the Parameter Π [2]

The ability to effectively estimate precipitable water is primarily determined by the accuracy to which we can estimate T_m. This is mainly attributed to the accurate characterization of the refractivity constants over the past half-century, resulting in the weighted mean temperature, T_m, being left as the dominant error source. Figure 2-4 displays the error in Π in relation to the error in T_m. The solid line represents experimentally determined errors in the nominal values of the atmospheric refractivity constants, and the dashed line represents double these nominal error values. It is apparent that even doubling the error in the refractivity constants k_1, k_2, and k_3 results in only a minimal offset in the Π parameter error relative to the change in the T_m error.
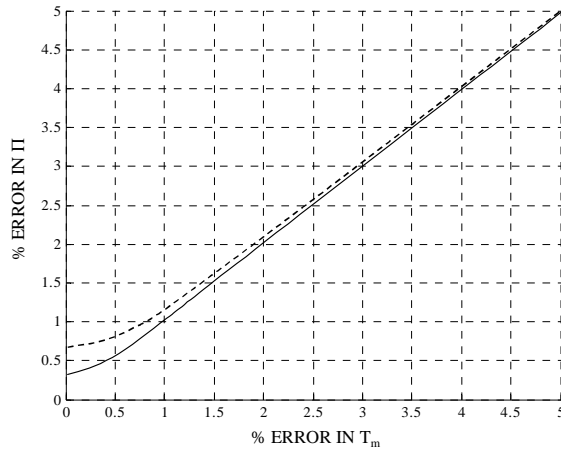
Figure 2-4. Variance in the Error of the Parameter Π [2]

It has been proven that the constant of proportionality, Π, can be determined to accuracies of 1-2%, depending upon the approach utilized [3]. A tuned value for the mean temperature T_m can be calculated using location dependent atmospheric regressions, as shown in the previous section by Equation 2-15. This regression has a 4.74 K rms deviation, producing a relative error of less than 2% [1].

2.4 Summary

It is clear that traditional methodologies have shortcomings that inhibit the effective use of the water vapor distribution in atmospheric monitoring and weather forecasting. Moreover, it has been established that additional, more accurate measurement methods will best allow for the accurate determination of atmospheric water vapor fields by supplementing these traditional methods. The Global Positioning System allows for an ideal supplementation, possessing characteristics with strengths where each traditional method proves insufficient. A methodology exists for effective and accurate atmospheric precipitable water determination via GPS, enabling accuracies

that meet or exceed those associated with traditional methods. Using this developed

methodology should make it possible to examine its ability to be employed in a variety of

situations and operational environments.

III. Methodology

3.1 Overview

This chapter describes an experimental GPS receiver network and the methods used to analyze precipitable water over that experimental network. The background and theory outlined in Chapters 1 and 2, respectively, merely serves as the basis for actual implementation. GPS precipitable water determination methods involve many additional contributing factors including peripheral data integration, estimation process strategies, and experimentation setup. More specifically, the implementation aspects studied in this thesis require further extension of the mathematical algorithms described in Chapter 2. This includes reinvestigating the factors contributing to effective GPS precipitable water determination, and the examination of degrading performance factors consistent with the thesis problem statement.

3.2 GPS PW Initialization

Precipitable water determination via GPS is essentially an estimation process, using satellite observations from a network of receivers, corresponding satellite ephemerides, established atmospheric constants, and surface atmospheric measurements. Initial consideration was given to developing custom software for the GPS data processing, which forms the basis of the research. However, the carrier-phase ambiguity resolution and tropospheric estimation algorithms would have required too large an effort for the time constraints associated with this research. As a result, several GPS data

processing software packages were considered. Utilizing a proven and established GPS processing software package was essential. In this thesis, the Bernese version 4.2 GPS software was chosen for the parameter estimation processes [5]. This software has been used throughout the world, particularly in the European and Southeast Asian communities, and has been proven to be accurate and effective in nearly all its applications.

3.2.1   Bernese GPS Software Familiarization

As the Bernese GPS software is the key tool used in this research, it was necessary to gain a working knowledge of how to set up and use this analytical tool. Although the software is a very powerful asset in the realm of GPS analysis, it has yet to be completely refined and user friendly. As a result, the Bernese software is not necessarily intuitive in its operation, and the improper implementation of the software could very easily lead to inaccurate or even unusable results in the GPS PW study.

Although the documentation or "users manual" that accompanied the software was extensive, it was written under the assumption that the user had previously attended the Bernese GPS software class. The program's developers teach this software familiarization class at the University of Berne in Switzerland. Initial efforts to learn the intricate nature of the Bernese software through the accompanying documentation manual were unfruitful, and further training was necessary. Taking the Bernese software class in Switzerland was deemed to be the best solution, since Bernese software use is somewhat limited in the United States region of the world.

The Bernese software class demonstrated that the process was iterative in nature, producing an accurate result only if each step of the analysis process was accomplished correctly. This is inherently problematic, as errors in early iterations can ripple through the process, compound with each other, and potentially produce very errant or inconsistent results. Understanding and familiarization with each iteration step proved to be critical in figuring out how to best employ the software. Moreover, the menu system utilized to provide the visual interface with the Bernese software proved to be a bit more intricate than initially perceived. The menu system itself serves as a link to thousands of subprograms and routines that actually perform the analysis, with each of these subprograms utilizing a variety of specific data files containing precise information that is analysis dependent. Setting up the Bernese software to use the proper information files was once again pivotal for proper and accurate program operation.

3.2.2   GPS Network Establishment

After familiarization with the Bernese software had been completed, a GPS receiver network had to be chosen for this research. Initially, the possibility of setting up receiver hardware to create our own GPS network from scratch was considered. However the funding and sheer magnitude of such a hardware implementation endeavor was deemed outside the research scope. The focus was turned to existing networks, particularly the Continuously Operating Reference Station (CORS) network [8].

Past encounters with the CORS network proved it to be very compatible for use in this precipitable water research. First, the receiver data is posted on the Internet and archived for years, leaving it readily accessible for processing [8]. Secondly, hundreds of

receiver sites exist in this network, spanning the 50 States, Guam, American Samoa,

Central America, and the Caribbean regions as shown in Figure 3-1.
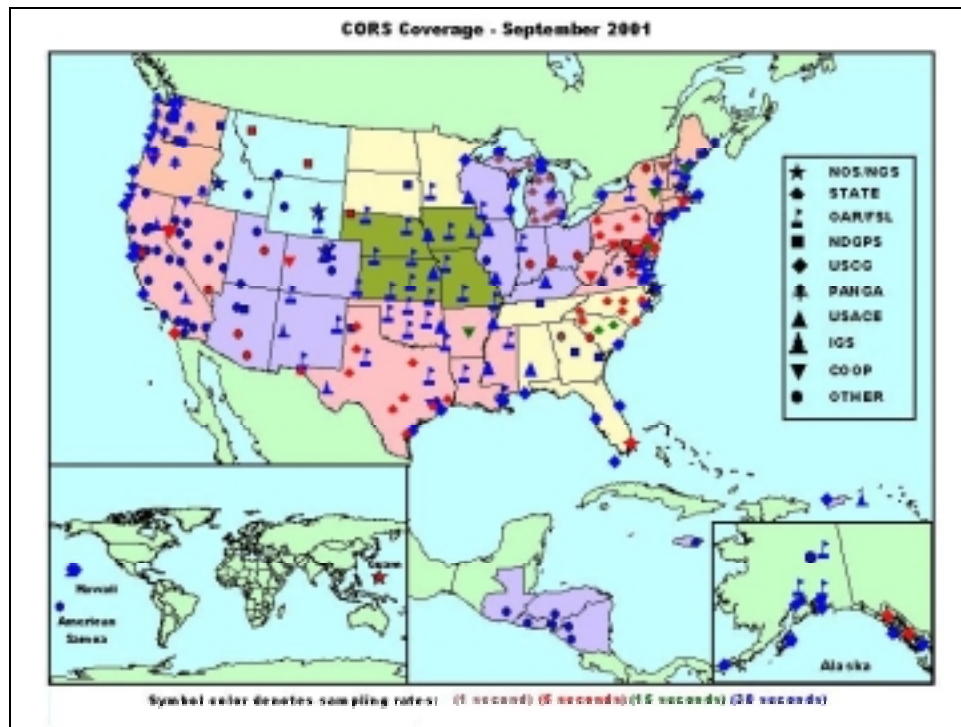
Figure 3-1. NOAA CORS Network [8]

However, one of the most attractive attributes of the CORS network lies in a

subset of CORS stations that have already been setup and utilized for the GPS estimation

of precipitable water. This subset of stations has its own GPS meteorology Internet site,

where it is possible to obtain atmospheric measurement data, tropospheric delays, and the

calculated PW in addition to the standard observation and ephemeris data found at the

CORS site [10]. This subset of GPS-MET reference stations is shown in Figure 3-2.

Figure 3-2. GPS Meteorology Network [10]

The subset of CORS sites used in the GPS meteorology field is ideal for use in

this study using the GPS-based PW calculation. The GPS meteorology stations provide

comparison data for the calculated hydrostatic delays, wet delays, and precipitable water,

all of which are fundamental to the research focus. Furthermore, the equipment models

at these GPS-met sites are very similar, enhancing the internal consistency of both the

GPS data and the corresponding atmospheric measurements. It is important to

understand that CORS GPS stations do not necessarily have the meteorological

equipment necessary to measure atmospheric conditions such as temperature and

pressure, which are necessary in the determination of precipitable water. However, the

GPS-MET subset of the CORS network does have the all the necessary atmospheric

measuring devices, and the data is posted on the CORS website as observed

meteorological files.

With the GPS-MET nationwide network in mind, a good regional network was sought out to accomplish the analysis. Since a major goal in this thesis was to evaluate precipitable water determination in a military context, present day operations in Afghanistan served as a good reference for gauging the scale of this thesis study. With the defined scale in mind, the GPS-MET network was examined to determine the best station grouping for this research. Both medium station baseline lengths of greater than 100 to 200 kilometers and an evenly spaced network that would ensure the best regional coverage for the GPS precipitable water research were sought out.

The main motivation for using medium station baseline lengths of greater than 100 to 200 kilometers was to achieve good results in both ambiguity resolution and tropospheric parameter estimation. Ideally, shorter baselines (i.e., 10-20 km) are least demanding on ambiguity resolution. This stems from the nearly identical tropospheric and ionospheric conditions seen by both station locations, resulting in the virtual elimination of the respective errors using double-differenced phase measurements. The elimination of the tropospheric and ionospheric errors leaves a minimal number of error terms that must be estimated to resolve the ambiguities [11]. Unfortunately, precipitable water is directly related to the tropospheric error, and GPS PW investigation is hindered by the elimination of this particular error term. As baselines increase in length, tropospheric and ionospheric errors become more prominent as a larger difference is observed in the atmosphere overlying the station locations. Ambiguity resolution becomes more difficult due to both the addition of increasing tropospheric and ionospheric error terms and their cross-correlation with the integer ambiguity values trying to be resolved. However, the increasing tropospheric error term and the difference

of the observed satellite elevations between stations results in better estimation of tropospheric parameters and, in turn, precipitable water over the locations.

With all of these considerations in mind, the central U.S. region looked ideal for the PW study. The states of Oklahoma, Kansas, Nebraska, Missouri, Illinois, Iowa, Wisconsin, and Minnesota comprised a GPS-MET station network that would best fit the baseline and spacing requirements and provide a good regional variety of weather patterns. The network can be seen in Figure 3-3, with the four-letter station designators chosen for the study highlighted and the country of Afghanistan superimposed to show the scale. Note that only the highlighted stations (BLRW, CNWM, FBYN, GDAC, HBRK, HKLO, HVLK, LMNO, LTHM, MRRN, NDS1, NLGN, PRCO, RWDN, SLAI, VCIO, WDLM, WNCI) are part of the research network.
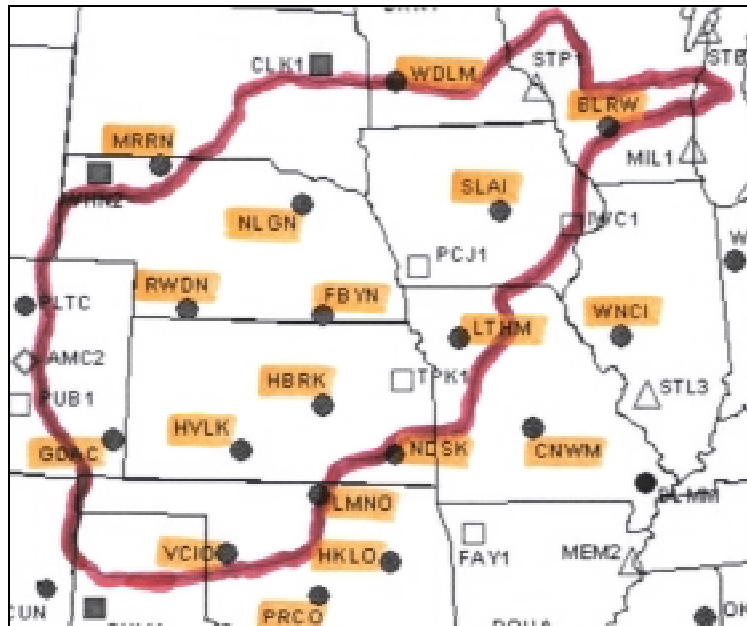
Figure 3-3. Thesis GPS Meteorology Network

Further consultation with meteorologists indicated that a good weather pattern for examination existed during the week of 7-13 July 2001. During this time period, a strong

weather system known as "The Ring of Fire" was moving across the central region of the

United States with significant thunderstorm activity. Taking their expertise into

consideration, the study converged on the central U.S. network described above during

this recommended time frame, hopeful that the weather activity would positively

contribute to the water vapor distribution research in this region.

3.2.3   Satellite Signal Area of Influence

Different GPS satellite elevations cause the GPS signals to transmit through

different parts of the Earth's atmosphere, as described in section 2.3.2. Meteorologists

indicate that most of the atmospheric moisture is within first 20 kilometers, and by setting

a satellite elevation cutoff of 10 degrees a region of influence is introduced to each

station location. Effectively, the GPS signals would traverse through the 20-kilometer

atmospheric moisture region within a 114-kilometer range of each station location, given

this 10-degree satellite elevation cutoff. Figure 3-4 shows how the regions of influence

for each station location interrelate with each other.
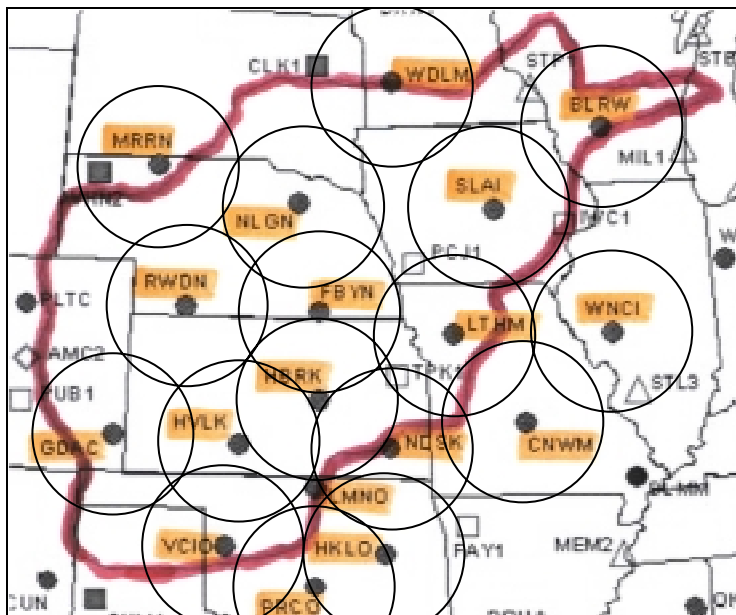
Figure 3-4. Thesis GPS Meteorology Network Regions of Influence

Throughout the research's data processing, a moderate satellite elevation cutoff of 10 degrees was used. Elevation cutoffs of more than 10 degrees would shrink each circle of influence, causing less overlap effect, whereas elevation cutoffs below 10 degrees would expand the circles of influence. A multiplicative effect is experienced as the elevation cutoff angle decreases. For example, a 10-degree cutoff has a 114-kilometer range of influence, whereas a 5-degree cutoff experiences a 228-kilometer range of influence. Slight overlap is ideal, as this would promote the characterization of all the tropospheric effects encountered throughout the network region.

3.3 Precipitable Water Determination via GPS

With the basis for the thesis research established, actual data processing using the Bernese GPS software began. The goals were to compare the results with previous GPS precipitable water calculations, and then investigate the limitations imposed in a military

context through the use of degraded orbits, a minimal set of available stations, and possible interpolation methodologies. The sections that follow describe the various steps taken to calculate precipitable water for the experimental network.

3.3.1   Network Coordinate Determination

The CORS GPS receiver network has published values for each station's coordinates. These published coordinates resulted from processing station data over time. The time intervals ranged from several weeks of continuous data to every day since the station's inception. The computed coordinates are transformed into a particular reference frame as defined by the International Earth Rotation Service (IERS), such as the most recent IERS Terrestrial Reference Frame (ITRF), with corresponding reference frame velocities. With this information, it is possible to take the coordinates at the reference frame epoch, and propagate them with the corresponding velocities to determine the predicted coordinates for the time period under examination.

It should be noted that these coordinates are not absolute truth, as they are calculated with varying data sets and updated on a yearly basis. This thesis will take these "published" coordinates and use them as a point of comparison for the stations in the experimental network. For the purposes of this study, the coordinates will primarily be estimated based on the data for the period of 7-13 July 2001. This estimation will allow for the best possible consistency throughout the PW study, ensuring continuity with the ambiguity and parameter resolution within the Bernese structure.

Proper and accurate coordinate determination is paramount due to the magnitude of the error term that drives precipitable water determination. PW is directly proportional

to the zenith wet delay at a particular receiver site, as seen in section 2.3.2. The wet delay term is very small, typically in the magnitude of 10 to 30 millimeters during the summer in the U.S. As a result, coordinate offsets of a few centimeters will significantly impact the accurate calculation of the induced atmospheric wet delay, thereby rippling into inaccurate PW determination.

To determine the coordinates for the week of 7-13 July 2001, observation data from each location in the 18-station network was processed with the Bernese GPS software. Special consideration and additional focus was given to the estimation of the station coordinates during the Bernese processing iterations. Precise GPS orbits were used, as they are the most accurate orbits available and capable of providing the necessary coordinate accuracy for the GPS PW thesis study. In an operational system, the precise orbit would not be available to determine network coordinates to the required accuracies, but the assumption here is that there would be enough time to accurately determine the coordinates before actual implementation. In this research the "published" NOAA CORS coordinates were used as initial rough estimates of the actual station locations, and the coordinates were estimated at each of the critical processing iterations. Taking on this strategy provided a good basis or starting point for the GPS PW study.

3.3.2   Tropospheric Delay Estimation

The Bernese GPS software does not have the built-in capability to calculate precipitable water explicitly. Furthermore, Bernese version 4.2 does not have an effective integrated capability that accurately separates the zenith wet delay from the total zenith tropospheric delay. After some initial brainstorming, two possible solutions were

posed. Either the Bernese software code could be modified to enable an integrated and automated calculation of PW, or the Bernese software could be utilized to accurately estimate the total zenith tropospheric delay and other MATLAB$^{®}$ code could be written to calculate PW from these total delay values. The latter option (utilizing MATLAB$^{®}$ code) was chosen for this thesis research. Bernese is written in FORTRAN, and lack of expertise in FORTRAN programming made the option to modify the Bernese software unappealing.

The Bernese GPS software has many features that allow for GPS data processing in many different modes. Regardless of the specific data, the Bernese software is based upon fundamental least-squares estimation processes implemented in a batch mode. The key observables used for the processing done in this research are the double-difference phase measurements [5]. Using these measurements it is possible to estimate a variety of parameters with the software. For typical users of this software, estimation of geodetic parameters such as station coordinates and their development in time are the main point of interest [5]. The importance of station coordinate estimation was evident, as it served as the basis for this research as previously described in section 3.3.1. Additionally, more obscure parameters can also be estimated once an established set of coordinates has been determined. In this research, the zenith tropospheric delay parameter was estimated for use in the calculation of precipitable water over each of the station locations.

The ambiguity resolution process is a significant portion of the GPS data processing. It is known that carrier-phase ambiguities are integer numbers, and resolving the ambiguity means to assign the correct integer numbers to the real-valued estimates [5]. Resolving and fixing the ambiguities on their true integer value makes the estimation

of other parameters considerably more accurate. Typically, the majority of the unknown parameters involved with the processing actually are the ambiguities [5]. There are various methods to resolve the ambiguities. A general two-step process can be used to describe most of them: estimate the ambiguities as real numbers along with other parameters, and reliably resolve the integer values of these estimations using statistical tests [5].

Using the station coordinates as described in the previous section, the data processing began to estimate the total zenith tropospheric delay. Careful consideration was given to determine the interval at which tropospheric delay was to be calculated, as increasing the number of estimates per day would result in an increase in the computational demands on the processing software and vice versa. Tropospheric delay estimates every 5 minutes may be ideal for near real-time PW estimation, but the speed of software computation speed may require the calculations on an hourly basis to get timely results. The surface meteorological data sampling was examined in conjunction with the calculation interval used by the NOAA GPS-MET demonstration network. An interval of 30 minutes was perceived to be the best choice, especially considering that the GPS-MET network utilizes the same 30-minute interval. This would allow for a point-by-point comparison between the two data sets.

Moreover, the 30-minute calculation interval would effectively demonstrate the various real-time effects while minimizing computational loading. For each time the precipitable water is to be calculated, the Bernese software must add an additional parameter to the state vector for each network receiver, which are then all estimated simultaneously. With a 30-minute calculation interval, the software must add 48

parameters in the state vector for each reference station per day, whereas 1-minute intervals would require 1,440 additional parameters per station per day. Such short estimation intervals would also result in extremely noisy precipitable water determination. This is primarily due to a lack of data to average over the short estimation interval, allowing errors to become more dominant. However, weather and atmospheric precipitable water can sometimes change quickly, especially during severe weather. Fortunately, severe weather only happens very occasionally, so normally weather conditions change more gradually. A 30-minute calculation interval allows for reasonable processing time and substantial data for evaluating the precipitable water determination over the given week.

There were several keys steps in the Bernese data processing procedure. First, optimum baseline combinations were utilized in forming the single difference solutions, using the number of observations as the optimization criteria [5]. Secondly, the quasi-ionosphere-free (QIF) algorithm [5] was employed to resolve the carrier-phase ambiguities. Finally, the ambiguities are treated as known values, to estimate only the tropospheric delays. The Neil mapping function was utilized to map the tropospheric delays to their equivalent zenith values [5].   These key considerations provided accurate estimation of zenith wet delay over each station within the examined network. Once accurate zenith troposphere delays had been estimated, MATLAB$^{®}$ code was developed to employ the precipitable water algorithm found in sections 2.3.4 and 2.3.5, using the meteorological data obtained from the CORS website. The resultant precipitable water values were used in data comparison and analysis processes described in the next section.

3.4 Experimentation Process

Once a method had been established to calculate the precipitable water across the network of 18 stations, further analysis was taken to determine the accuracy of these values. After analyzing the best-case network scenario, two degraded cases were investigated. First, orbit degradation was introduced to see how less accurate, real-time orbits affect the accuracy of GPS precipitable water estimation. Secondly, network degradation was performed to examine how effectively a minimal set of stations can resolve the precipitable water at those locations (simulating the case where you are unable to place receivers in enemy territory). Both degradations were first analyzed independently, and then the effects of both degradations together were evaluated. Additionally, an analysis of interpolation methods was performed to see how well PW values could be interpolated in the degraded network case. Each of these analyses required all of the necessary data for calculating precipitable water (surface meteorological measurements and valid zenith tropospheric delay) to be available at each investigation time. Instances with a lack of any of these data elements were excluded from the study. The results of the analyses are presented in Chapter 4.

3.4.1 Initial Validation

Initial analysis was performed using the full 18-station GPS meteorology network with precise orbits. The goal of this initial analysis was to verify that the algorithm employed in this research produces results similar to other validated data. The comparison data used for this initial validation was from NOAA's GPS-MET network. Tropospheric delays for the 18 stations were compared to verify that the Bernese

software was properly utilized in the estimation process. Without good zenith tropospheric delay estimates, the precipitable water calculation would be inherently errant. An exact match was not expected, but rather equivalent magnitudes and small relative differences were the primary objectives. Next, the surface meteorological measurements for pressure and temperature were compared between the sources. These surface parameters are utilized within the GPS precipitable water algorithm, and significant discrepancies would adversely affect the accuracy of this calculation.

Finally, the calculated precipitable water was compared with the NOAA GPS-MET precipitable water estimates. Again, an exact match was not expected, primarily due to the differences in GPS processing software, data files, and NOAA's more advanced GPS-MET algorithms. However, the same magnitude and small relative differences were the objective. Once this initial analysis provided ample verification for the research process, the full 18-station/precise orbit network results could be used as the truth basis for the remainder of the experimentation. In theory, the use of the full 18-station network with precise orbits gave the most accurate results achievable via the employed algorithm. Therefore, process consistency and uniformity were achieved by comparing all subsequent experimentation with the full 18-station/precise orbit network results.

3.4.2 GPS Orbit Degradation Examination

With the focus of making the precipitable water estimation process as close to real-time as possible, only GPS satellite ephemerides with real-time capability were investigated (in addition to the precise ephemeris). First, the utilization of the broadcast

ephemeris was examined, as it is the most accessible of the available ephemerides. Significant degradation was expected in the ability to determine precipitable water, as the broadcast orbits are the least accurate of those available. Given that broadcast orbits are calculated once per day with different windows of validity, near real-time implementation could easily be simulated by downloading it once and using in conjunction with the entirety of the data for that day.

Secondly, the IGS ultra-rapid ephemerides were used to examine the performance of a more accurate real-time orbit that has a more limited accessibility. The accessibility limitations stem from the requirement for self-production of a predicted orbit product comparable to the IGS ultra-rapid orbit, as the IGS ultra-rapid orbit solution is only available twice daily with a 9-hour delay. Near real-time implementation was simulated by using the ultra-rapid predicted orbit calculated at the beginning of each day of the examination week. In effect, this should show the worst accuracy possible using the ultra-rapid orbit, as its accuracy would increase if it could be updated at intervals throughout the day.

Although a degraded accuracy in precipitable water determination was expected in comparison to the precise orbit results, it was uncertain how much accuracy would be sacrificed using these less accurate real-time orbits. Moreover, the ability for the Bernese software to process the data given less accurate ephemerides was also investigated, particularly with respect to tropospheric parameter estimation.

3.4.3   Network Degradation Examination

The next analysis step was to examine the effects of a limited number of data

sources, and the corresponding network geometry. This allowed insight into the

effectiveness of the data processing algorithms within the Bernese software. Ambiguity

resolution and parameter estimation are both impacted by loss of available data used in

the processing. In particular, the investigation was based on having a minimal network of

perimeter stations, without access to observation data in the network's central region as

shown in Figure 3-5. The primary motivation for this case was based on the inability to

easily place receivers in enemy territory, which is a significant constraint present in most

military operational environments. Note that only the highlighted stations (BLRW,

CNWM, GDAC, MRRN, PRCO, WDLM, WNCI) were included in the degraded

perimeter network.

Figure 3-5. Degraded Thesis GPS Meteorology Network

Analysis was done using precise orbits, to see the effects less observation data and limited geometry had on the ability to estimate the precipitable water at each of the 7 perimeter stations. This analysis, in itself, does not investigate precipitable water determination over the entire network region. Those aspects concerning network resolution aspects are included in the analysis described by section 3.4.5.

3.4.4   Combination of Degradation Effects

Once the effect of minimal data availability and network geometry had been evaluated, coupling effects of introducing degraded orbits to the 7-station perimeter network were examined. Both the broadcast and ultra-rapid orbits were employed to quantify the effect of real-time implementation in conjunction with a minimal set of available observation data. Key concerns involve the increasing demands on the processing software regarding the ambiguity resolution and tropospheric parameter estimation processes, as the errors introduced by both the network and orbit degradations will be compounded together. The main question is whether or not this compounding error will be significant for the purposes of estimating atmospheric precipitable water.

3.4.5   Examination of Interpolation Methods

A final, and capstone, examination was the investigation of the ability to interpolate the water vapor field over the region using the 7-perimeter station network. This is where operational military restrictions in network density began to be taken into consideration. Both linear and cubic interpolation schemes were initially taken into consideration, as they were functions within MATLAB® and easily implemented.

Quantification of the "goodness" of the interpolation was done by statistically comparing the known values at the stations with the perimeter network and the interpolated values at those points. Only periods with all the required data available could be investigated, which included PW data at all 7 perimeter stations and corresponding actual PW values for each of the interpolated values. Invalid data at any one of the 7 perimeter stations would alter the interpolation over the entire network, skewing the results.

In order to eliminate cross-correlated effects of the degraded perimeter network PW estimation and the network interpolation of PW, a second investigation used values for the perimeter stations taken from the full 18-station network estimation case. This case would effectively eliminate the difference between the actual and interpolated values at those 7 perimeter stations, as the remainder of the network region is interpolated based on these "known" values. The interpolation error was isolated and quantified by itself through this analysis process.

Finally, the interpolation effect of having one centrally located station in addition to the perimeter network was investigated. The stations included (BLRW, CNWM, FBYN, GDAC, MRRN, PRCO, WDLM, WNCI) are highlighted in Figure 3-6.
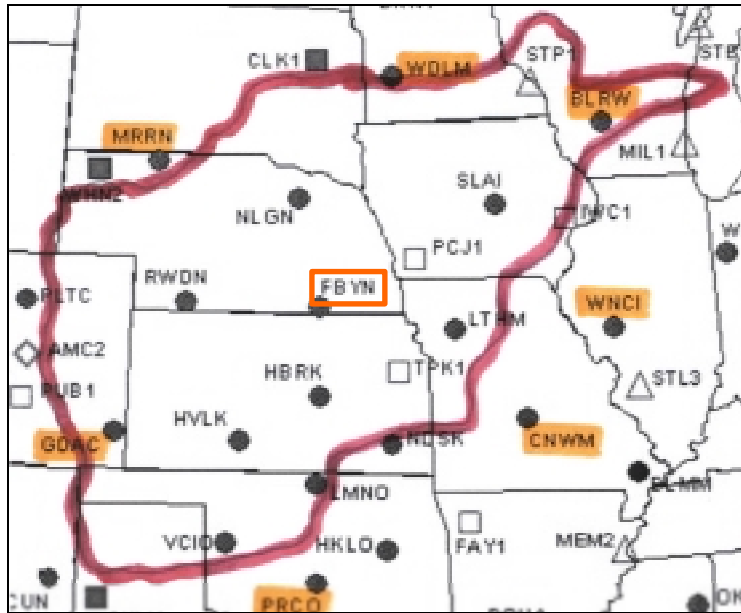
Figure 3-6. Complimented Thesis GPS Meteorology Network

This would primarily investigate trade-offs involving a slight increase in precipitable water resolution over the network region, while maintaining more limiting practical military operational restrictions.

3.5 Summary

This chapter discussed the overall processes and techniques used in this thesis. Establishment of a research network and choosing adequate GPS data processing software were important first steps of the investigation. Furthermore, estimating the network coordinates and tropospheric delays provided the means to determine precipitable water over each station in the network region. The experimentation process started with an initial validation of results, and then proceeded with an investigation of orbit and network degradation effects. Finally, network PW interpolation was

investigated using the degraded network to investigate potential military operational

factors and considerations.

IV. Results and Analysis

4.1 Overview

This chapter focuses on the results of the experimental processes as described in Chapter 3. Quantification of the results using both graphical and statistical methods provides insight into the GPS derived precipitable water behavior. These results are used to make inferences, conclusions, and recommendations about GPS precipitable water estimation processes.

4.2 Experiment Initialization

A good research basis was initially established using fundamental process investigation. First, coordinates for each station within the experimental GPS-PW network had to be determined. This was a crucial step that would effect all subsequent evaluation, as coordinate errors directly impact the quality of the results. Secondly, validation of the methodology had to be accomplished. The results of the employed algorithm had to be consistent with other comparable atmospheric precipitable water estimates, particularly the NOAA GPS-MET PW data. This would, in-turn, ensure a solid basis for more specific study and evaluation.

4.2.1 Network Coordinate Determination

As discussed in Chapter 3, the National Geodetic Service estimates station coordinates and velocities on a yearly basis with varying data sets and reliability. Recall

that some stations use data sets including every third day of data since initialization, where others may take three consecutive weeks of recent data. When the coordinates are estimated, they are typically put in a reference epoch to standardize the results amongst the different stations. The latest NGS ITRF97 coordinates for the stations within the experimental network as shown in Table 4-1.

**Table 4-1. ITRF97 Station Coordinates and Velocities (Epoch 1997.0)**

STATION	X (m)	VX (m/yr)	Y (m)	VY (m/yr)	Z (m)	VZ (m/yr)
BLRW	-43118.8630	-0.0164	-4654409.4640	-0.0011	4346305.2630	-0.0014
CNWM	-238909.2940	-0.0147	-5059509.1570	-0.0096	3863793.2900	-0.0022
FBYN	-622116.3610	-0.0154	-4847771.6530	-0.0010	4084781.3970	-0.0035
GDAC	-1065179.5840	-0.0144	-4934984.8990	-0.0001	3886468.7780	-0.0053
HBRK	-636268.5050	-0.0140	-4971311.2010	-0.0003	3932291.5460	-0.0058
HKLO	-529863.4700	-0.0137	-5159629.7220	-0.0013	3699768.3680	-0.0042
HVLK	-800338.2030	-0.0144	-4992906.7800	-0.0008	3875267.3060	-0.0065
LMNO	-666736.9160	-0.0140	-5077560.9640	-0.0009	3789624.4020	-0.0053
LTHM	-357996.9210	-0.0153	-4910005.6890	-0.0010	4041974.4560	-0.0026
MRRN	-948739.9470	-0.0160	-4582734.1410	-0.0009	4320380.7720	-0.0060
NDS1	-495849.8010	-0.0157	-5055714.8410	-0.0020	3844210.0140	-0.0046
NLGN	-641817.7130	-0.0161	-4688244.6030	-0.0010	4262977.8740	-0.0035
PRCO	-684650.0860	-0.0133	-5186967.8590	-0.0014	3636211.8820	-0.0058
RWDN	-903473.3010	-0.0154	-4802868.9530	-0.0009	4085854.5850	-0.0045
SLAI	-306731.4870	-0.0160	-4744691.8370	-0.0010	4237584.6280	-0.0023
VCIO	-826818.0220	-0.0140	-5095172.2770	0.0009	3734993.1880	-0.0048
WNCI	-431414.7100	-0.0168	-4522955.6570	-0.0011	4461724.5320	-0.0027
WDLM	-40910.1950	-0.0153	-4916498.6230	-0.0010	4049479.2990	-0.0014

In order to maintain consistency throughout the research, it was in the best interest to estimate the network stations' coordinates from the GPS measurements, and to only use the NGS ITRF97 solution as a source of comparison. Using the 7-day data set spanning 7-13 July 2001, used throughout the research process, coordinates were estimated for each of the 18 stations in the experimental GPS-PW network. Precise orbits were utilized to maximize the accuracy of the coordinate estimation, as small coordinate offsets would significantly effect estimation of small error parameters such as tropospheric delay. Coordinates were first estimated for each day, and then for the entire

week. The daily estimates were allowed to converge upon a floating solution with a
constraint placed upon the station BLRW, whereas, the final estimate for the week fixed
station BLRW at its reported ITRF97 position. Initial comparison yielded final results
showing errors in excess of 40 to 50 cm. Every station in the network appeared to have
the same fluctuation in the daily coordinates, displayed by typical examples in Figures 4-
1 and 4-2.
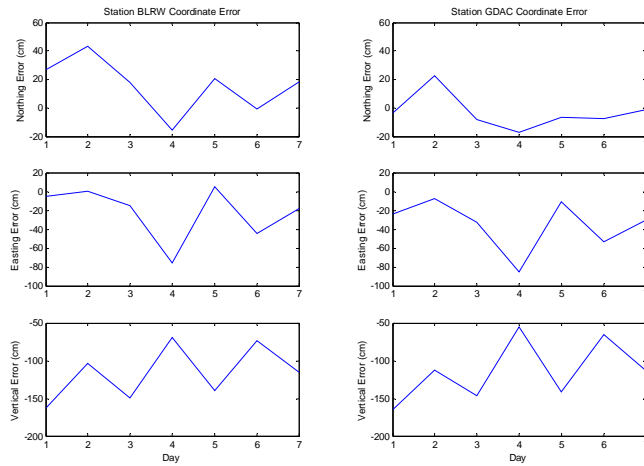
**Figure 4-1. Initial BLRW and GDAC Coordinate Errors
(Daily Results – Weekly Results)**
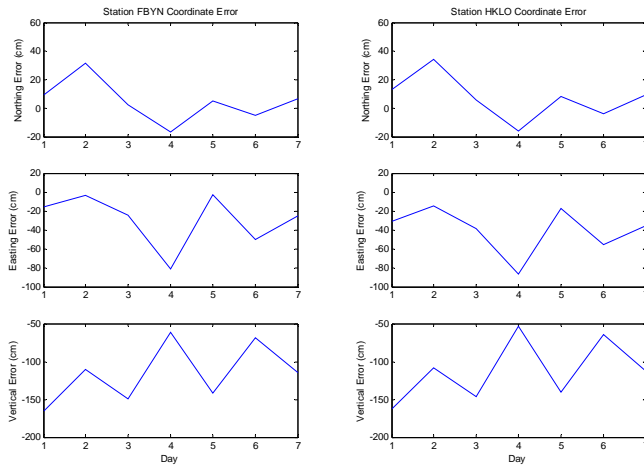
**Figure 4-2. Initial FBYN and HKLO Coordinate Errors
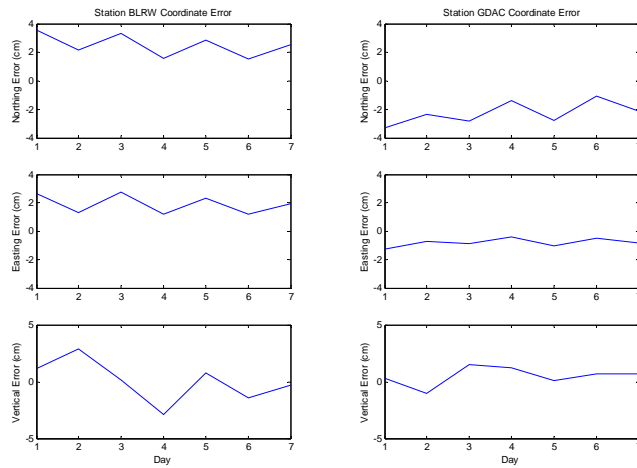(Daily Results – Weekly Results)**

The corresponding three-dimensional error statistics for these coordinates are shown in Table 4-2. The error is consistent and uniform throughout all 18-stations.

Table 4-2. Initial 7-Day Coordinate Comparison 3-D Error Statistics
(Daily Results – Weekly Results)

	MEAN (cm)	STD (cm)	RMS (cm)
OVERALL	125.60	26.482	128.34

The vertical error was poorest, with each component proving to be much larger than expected. An error vector greater than a meter is grossly insufficient for effective precipitable water estimation. Further consultation recalled that the daily coordinates were allowed to float within a constraint window and the final results were fixed on a selected station, a random network offset was suspected to be responsible for the large positioning errors. This would explain the striking similarities in positioning observed between all of the stations, as each set of plots in Figures 4-1 and 4-2 appears to be nearly identical. The network geometry, or relative positions of stations throughout the network, should be significantly more consistent. To eliminate the random daily network offsets, an adjustment technique was applied to each set of daily coordinates. Essentially, the centroids for each of the daily and final coordinate solutions were calculated, and the relative difference between each of the daily centroids and the final centroid was subtracted from all 18 of the corresponding daily coordinates. Through this process a much more consistent set of coordinates was obtained, varying in the 1 to 2 cm range, as seen in Figures 4-3 and 4-4.

**Figure 4-3. Offset Eliminated BLRW and GDAC Coordinate Errors
(Daily Results – Weekly Results)**
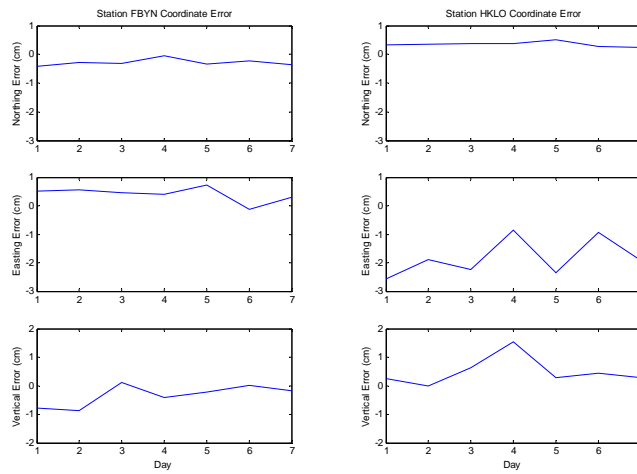
**Figure 4-4. Offset Eliminated FBYN and HKLO Coordinate Errors
(Daily Results – Weekly Results)**

The corresponding error vector statistics for these coordinates are shown in Table 4-3. Both the station-specific and overall statistics are shown, displaying the small relative errors that exist at each network station.

**Table 4-3. Offset Eliminated 7-Day Coordinate Comparison 3-D Error Statistics
(Daily Results – Weekly Results)**

STATION	MEAN (cm)	STD (cm)	RMS (cm)
BLRW	3.6616	0.71669	3.7212
CNWM	2.0496	0.63299	2.1317
FBYN	0.68581	0.29350	0.73768
GDAC	2.5961	0.76750	2.6915
HBRK	0.67934	0.29408	0.73186
HKLO	2.0166	0.51810	2.0729
HVLK	1.4754	0.34292	1.5092
LMNO	1.7889	0.84651	1.9531
LTHM	1.1355	0.36409	1.1845
MRRN	2.9071	0.88655	3.0207
NDS1	1.1989	0.31486	1.2338
NLGN	1.7391	0.46048	1.7906
PRCO	2.4710	0.52189	2.5178
RWDN	1.8649	0.59072	1.9434
SLAI	2.0194	0.54183	2.0808
VCIO	2.2680	0.50557	2.3158
WDLM	3.2182	0.69376	3.2817
WNCI	2.7388	0.75850	2.8274
OVERALL	**2.0286**	**0.97174**	**2.2476**

Now each network station appears to have more consistent, smaller variation. This is evident in both the graphical and statistical analyses. Two main contributing factors were thought to be responsible for these variations in estimated coordinates. First, only one week of observation data was processed to estimate the network coordinates. A longer period of investigation would produce more stable and accurate estimation, resulting from the averaging of increased amounts of available data. Secondly, the observation data from the investigation period of 7-13 July 2001 might have had more bad observation data than usual. The quality of observation data can be resolved using longer investigation periods as discussed previously.

Further investigation into resolving coordinate accuracy issues was minimal, as time constraints limited inclusion of further data screening and additional days of observation data. Fluctuations of several centimeters were deemed suitable given the

resources at hand. The final ECEF coordinates used throughout the research are

displayed in Table 4-4.

Table 4-4. Estimated ECEF Station Coordinates

STATION	X (m)	Y (m)	Z (m)
BLRW	-43118.9371	-4654409.4690	4346305.2567
CNWM	-238909.3564	-5059509.1892	3863793.2823
FBYN	-622116.4267	-4847771.6612	4084781.3855
GDAC	-1065179.6342	-4934984.9166	3886468.7579
HBRK	-636268.5542	-4971311.2248	3932291.5280
HKLO	-529863.5196	-5159629.7343	3699768.3501
HVLK	-800338.2517	-4992906.8001	3875267.2799
LMNO	-666736.9689	-5077560.9765	3789624.3860
LTHM	-357996.9820	-4910005.6971	4041974.4507
MRRN	-948740.0092	-4582734.1528	4320380.7461
NDS1	-495849.8570	-5055714.8601	3844210.0033
NLGN	-641817.7770	-4688244.6111	4262977.8634
PRCO	-684650.1308	-5186967.8854	3636211.8647
RWDN	-903473.3596	-4802868.9639	4085854.5726
SLAI	-306731.5543	-4744691.8449	4237584.6214
VCIO	-826818.0664	-5095172.2881	3734993.1695
WNCI	-431414.7748	-4522955.6677	4461724.5185
WDLM	-40910.2706	-4916498.6242	4049479.2958

A check was performed to see how the estimated coordinates compared to the NGS

ITRF97 coordinate set. This would ensure that the estimated coordinates are reasonable.

No significant differences were present in any one particular station, as all had similar

relative offsets. The statistics are displayed in Table 4-5.

**Table 4-5. Estimated vs. ITRF97 Coordinates 3-D Error Statistics
(Estimated – ITRF97)**

	MEAN (cm)	STD (cm)	RMS (cm)
OVERALL	1.5107	0.7735	1.6874

With an established set of network coordinates, the precipitable water investigation

began. The estimated network coordinates shown in Table 4-4 were used throughout the

remainder of the research.

4.2.2   Initial Methodology Validation

To validate the PW algorithm used within this thesis, initial results were compared to the NOAA GPS-MET PW estimates. As described in Chapter 3, precise orbits were used to obtain the best possible experimental estimates for this initial validation. Comparison showed very little difference between network stations, with typical station results for the entire week shown in Figures 4-5 and 4-6.
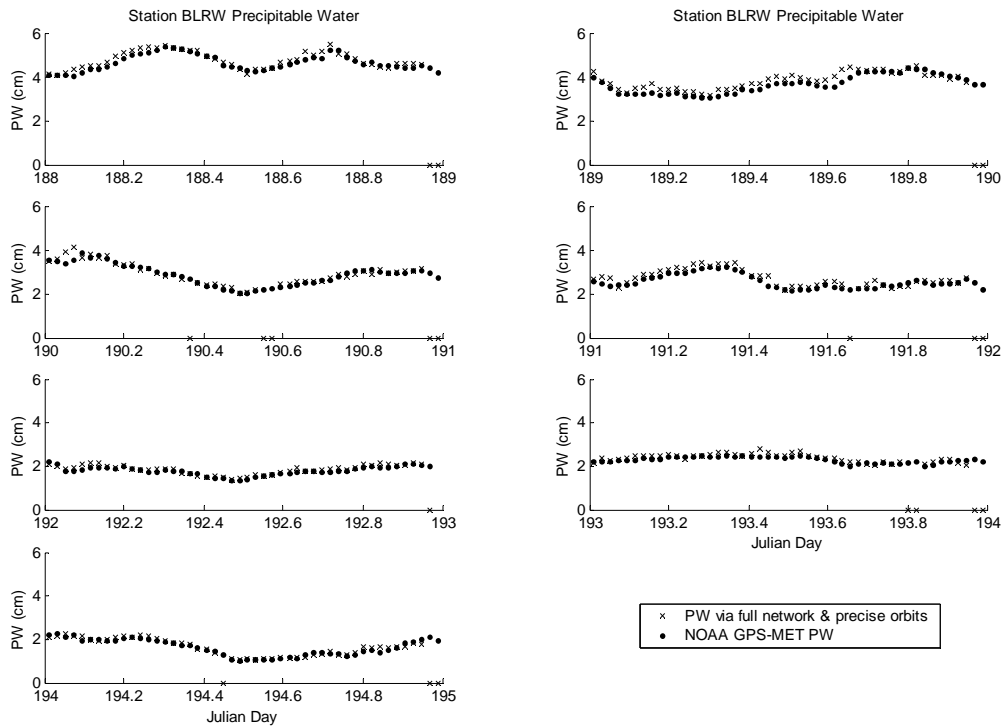
Figure 4-5. BLRW Experimental vs. NOAA GPS-MET PW
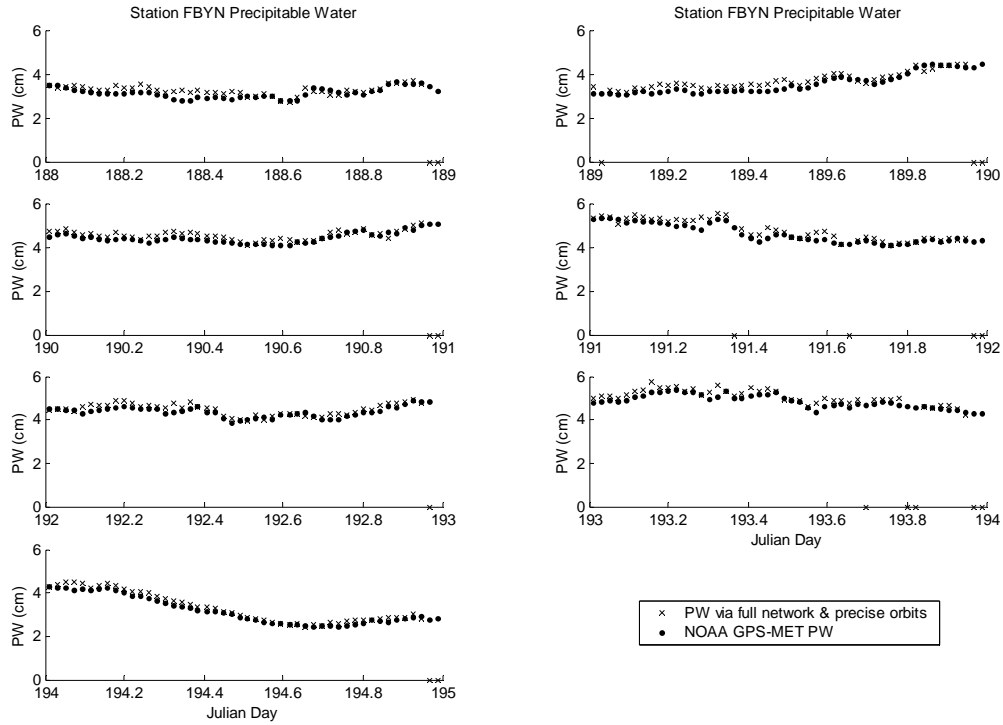
Figure 4-6. FBYN Experimental vs. NOAA GPS-MET PW

Each day of the week was examined to check for any significant data problems or problematic station locations. PW estimation performance was consistent throughout the examination period, with small relative errors. There appeared to be very few station-specific factors, so daily and weekly statistics best characterize performance, as shown in Table 4-6.

Table 4-6. Experimental vs. NOAA GPS-MET PW Statistics
(Experimental Results – NOAA Results)

Day	MEAN (cm)	STD (cm)	RMS (cm)
188	0.15487	0.15159	0.21664
189	0.20159	0.16126	0.25808
190	0.13196	0.12992	0.18511
191	0.22001	0.17334	0.28002
192	0.12259	0.16897	0.20866
193	0.18438	0.14814	0.23645
194	0.16353	0.16136	0.22966
OVERALL	**0.16817**	**0.16055**	**0.23249**

4-9

With the results accurate to within 2.0 mm, adequate validation was achieved for the thesis GPS precipitable water methods. The mean indicates that there is a about a 1.7 mm bias to the experimental PW estimations. Consistent trends are indicated by the standard deviation of about 1.6 mm. Overall accuracy is shown via RMS, which is about 2.3 mm and very representative of the consistent small differences seen throughout the comparison. Note that instances were excluded from the statistics when PW values were not available concurrently from both sources. This is the standard procedure throughout the remainder of the analysis process.

The differences between the experimental and NOAA GPS-MET precipitable water results can be the result of several factors. First, different processing software used by the NOAA GPS-MET system could potentially render slight differences in precipitable water values. Secondly, NOAA uses an ephemeris of equal accuracy to the IGS ultra-rapid orbit. By using a more accurate ephemeris such as the precise orbit, the experimental results could potentially be closer to the true value of precipitable water. Lastly, the variance of the estimated network coordinates, discussed in the previous section, might also be responsible for adding slight errors in the precipitable water calculations.

Nonetheless, the results of the validation demonstrated very good consistency between the Bernese results generated in this research and the results obtained independently from a different group using different software. With the full-network with precise orbits analysis proven, it served as the basis for comparing the remainder of the PW determination investigation.

4.3 Degradation Investigation

Once the fundamental basis had been established through estimation of the network coordinates and initial methodology validation, investigation into the central thesis topics began. Two major degradations were investigated. First, orbit degradation was done to examine how precipitable water estimations are affected by reduced ephemeris accuracies. In particular, broadcast and IGS ultra-rapid orbits were used, because they are both near real-time products. Then, network degradation was done to evaluate the ability to estimate PW with data availability and network geometry limitations. Lastly, combining the degradation effects was examined to see how compounding errors affect PW estimation performance.

4.3.1 GPS Orbit Degradation Examination

The most easily accessible real-time orbit product is the broadcast orbit. Just as accurate station coordinates are required to properly estimate small error terms, satellite position accuracies are similar in their impact. Because the error of broadcast orbits is quite large (~260 cm), significant variations in the precipitable water estimation were expected and observed. In the broadcast orbits analysis, all stations within the full 18-station network had consistent results, with typical station results for the week displayed in Figures 4-7 and 4-8.
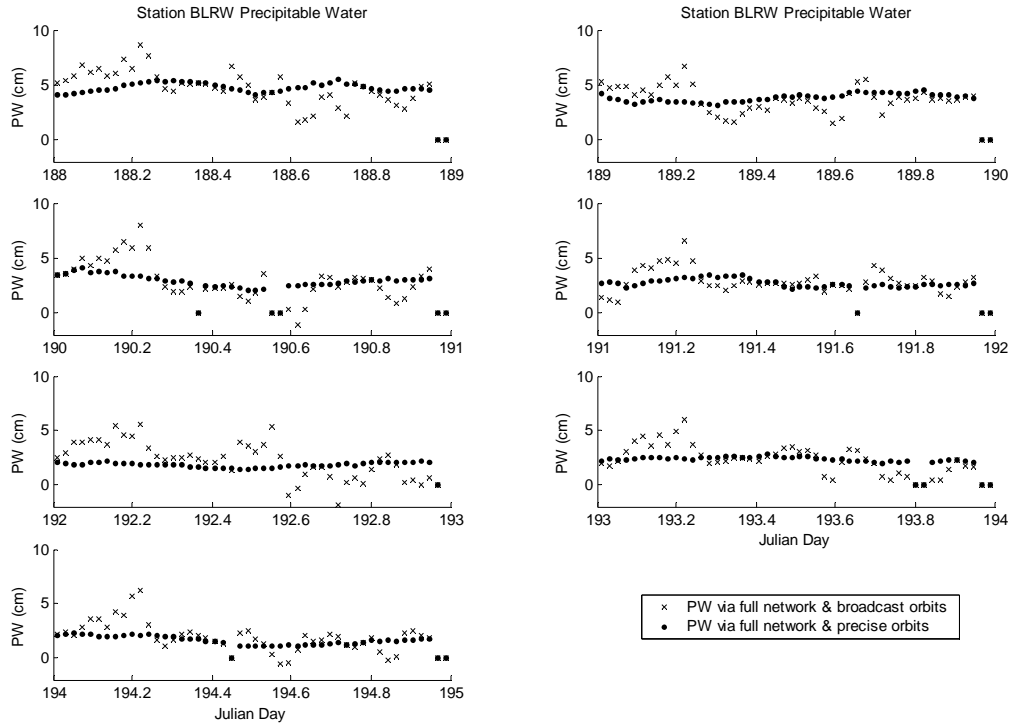
Figure 4-7. BLRW Broadcast Orbits vs. Precise Orbits PW Results
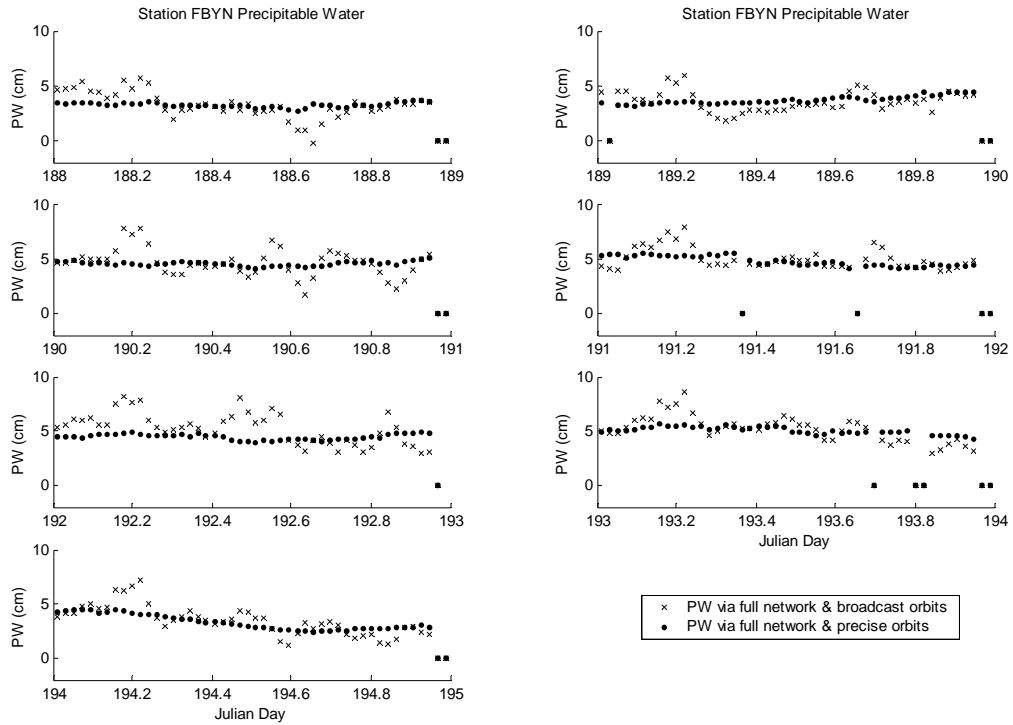
Figure 4-8. FBYN Broadcast Orbits vs. Precise Orbits PW Results

4-12

It is evident that inaccuracies present in the broadcast ephemeris causes significant variation in precipitable water estimation. The error statistics for PW obtained from using broadcast orbits (considering the precise orbit results as truth) are shown in Table 4-7.

Table 4-7. Broadcast Orbits vs. Precise Orbits PW Error Statistics
**(Broadcast Results – Precise Results)**

Day	MEAN (cm)	STD (cm)	RMS (cm)
188	-0.014775	1.2610	1.2603
189	-0.027911	1.0757	1.0753
190	0.10728	1.3177	1.3211
191	0.29755	0.90645	0.95342
192	0.86856	1.6495	1.8632
193	0.16570	1.0247	1.0372
194	0.18967	0.0176	1.0344
OVERALL	0.22491	1.2379	1.2581

The 2.2 mm mean indicates a slight bias, but by itself fails to give adequate insight into the true effects due to using broadcast ephemerides. The 1.23 cm standard deviation (STD) indicates a very variant PW data set. When 2-5 cm is the normal precipitable water range over the region, estimations with more than one centimeter errors will undoubtedly prove inadequate. The root-mean-squared value (RMS) of more than 1.25 cm adds to the overwhelming indication of poor overall accuracy. Thus, the broadcast ephemeris would be unsuitable for use in precipitable water estimation.

IGS ultra-rapid orbits provide an order of magnitude of increased accuracy, with a near real-time capability. With increased accuracy relative to the broadcast ephemeris, less variation in PW estimation was expected. Again, all stations within the full 18-station network had consistent results, and typical stations for the week are displayed in Figures 4-9 and 4-10.
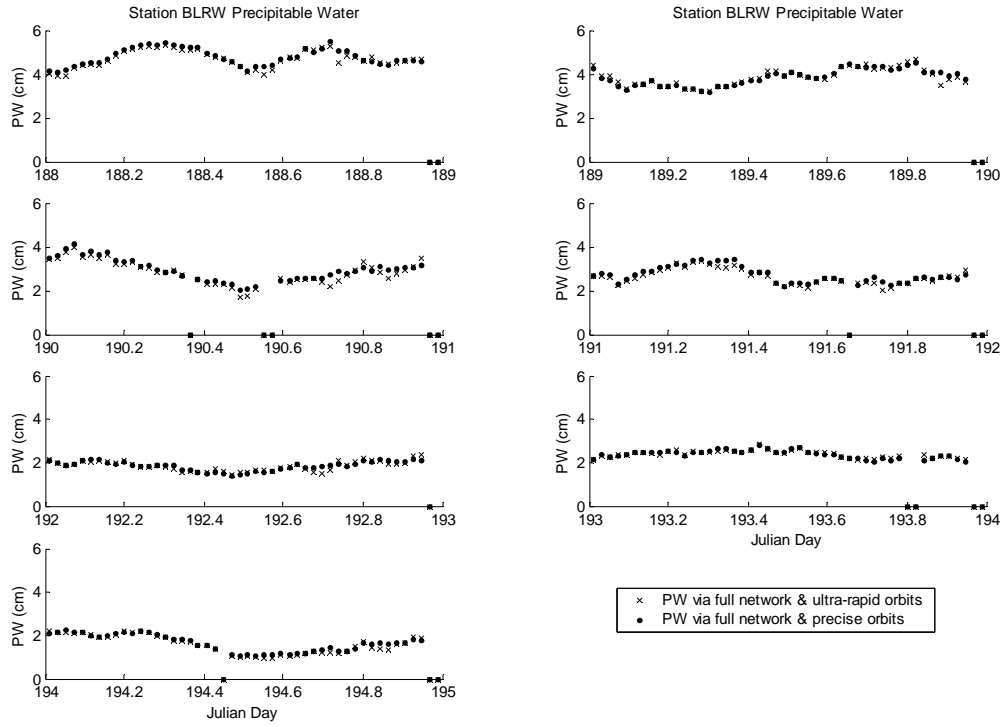
Figure 4-9. BLRW Ultra-rapid Orbits vs. Precise Orbits PW Results
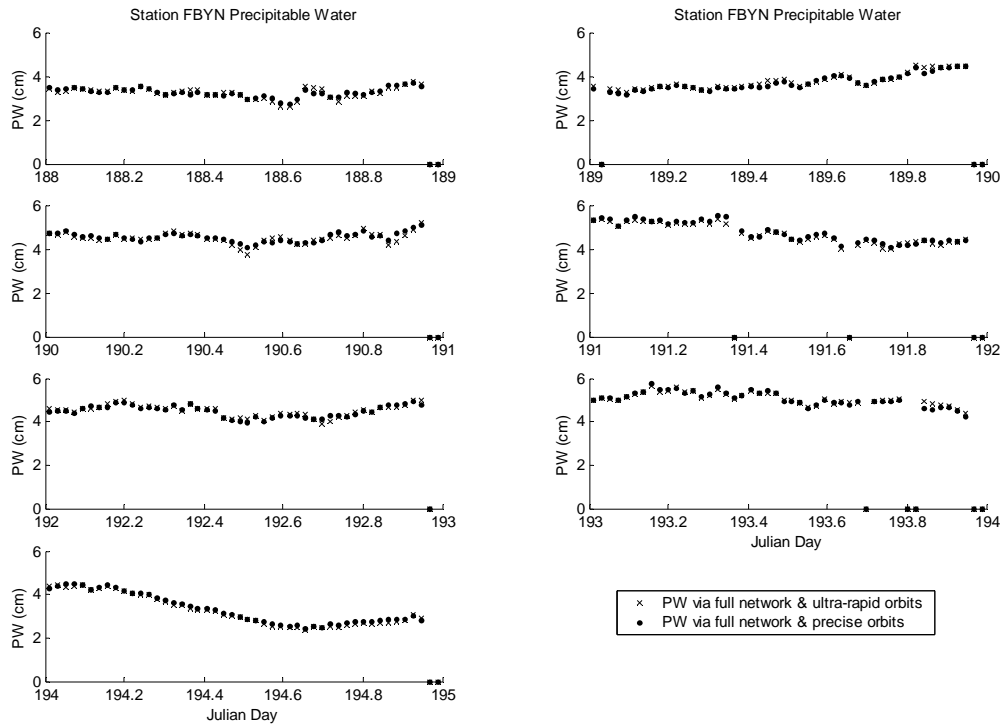
Figure 4-10. FBYN Ultra-rapid Orbits vs. Precise Orbits PW Results

4-14

Notice the small relative errors and significant improvement in the ability to estimate

precipitable water. The error statistics for PW obtained using IGS ultra-rapid orbits

(considering the precise orbit results as truth) are shown in Table 4-8.

Table 4-8. Ultra-rapid Orbits vs. Precise Orbits PW Error Statistics
**(Ultra-rapid Results – Precise Results)**

Day	MEAN (cm)	STD (cm)	RMS (cm)
188	-0.027467	0.11523	0.11838
189	0.036583	0.084227	0.091773
190	-0.036865	0.15149	0.15580
191	-0.045544	0.092235	0.10281
192	0.051236	0.10324	0.11518
193	-0.0055161	0.096497	0.096578
194	-0.056703	0.076401	0.095100
OVERALL	**-0.012213**	**0.11208**	**0.11273**

The statistics for precipitable water determined via the ultra-rapid predicted orbit

are very favorable. The mean reveals an almost negligible bias of about 0.1 mm. Both

the standard deviation and RMS values of about 1.12 mm indicate a very stable data set

and excellent overall accuracy. Additionally, the statistics may have been slightly better

if the statistics for day 190 were improved. The slight increase in standard deviation and

RMS was mainly attributed to two errant data points that were included. These errant

points were most likely caused by errors within the actual ultra-rapid predicted orbit.

The improvement in precipitable water estimation gained from using ultra-rapid

orbits is consistent with the order of magnitude improvement in orbit accuracy relative to

broadcast orbits. More importantly, it has a minimal loss of accuracy when compared to

PW estimation via precise orbits. Ultra-rapid orbits, or a similarly accurate predicted

orbit product, have the potential to provide the accuracy required for effective

characterization of precipitable water on a near real-time basis.

4.3.2   Network Degradation Examination

In addition to orbital accuracy degradation, limited data sources and network geometry are also important factors when considering military implementation. Although increased numbers of stations will inherently provide better estimation, this is not always possible in real operational environments. Therefore, lack of observation data and longer network baselines should render less accurate estimation of PW at the included stations. The perimeter network shown previously in Figure 3-5 was used in this network degradation examination. Precise orbits were used in order to quantify the network degradation effect without the introduction of other error sources. Consistent performance was seen amongst all stations in the degraded perimeter network. Typical examples are shown in Figures 4-11 and 4-12.
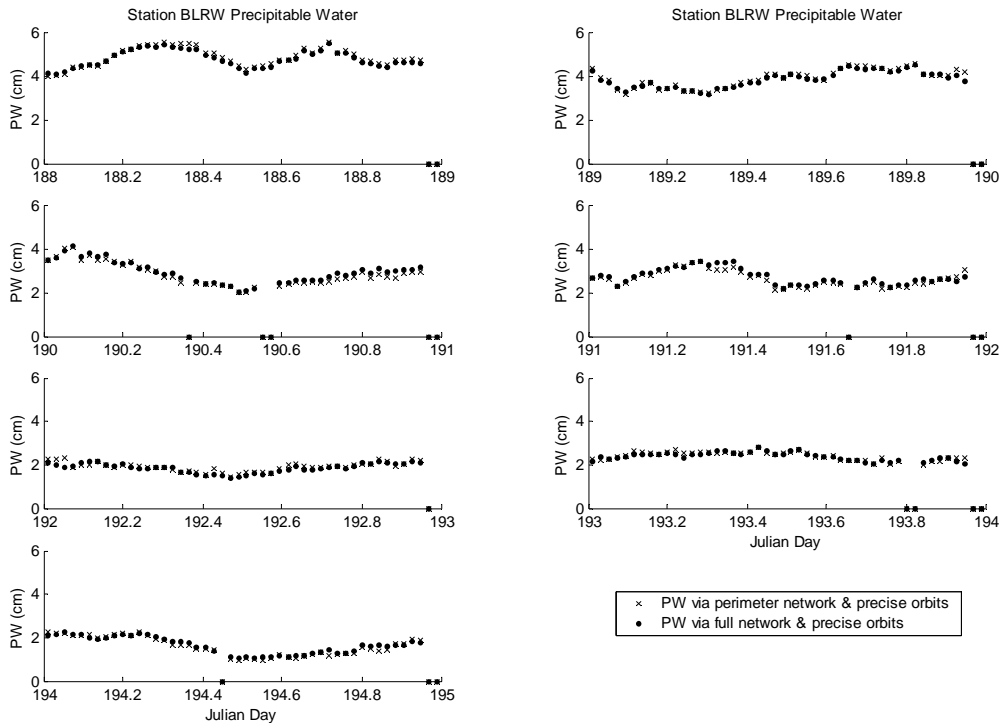
Figure 4-11. BLRW Degraded Network vs. Full Network PW Results
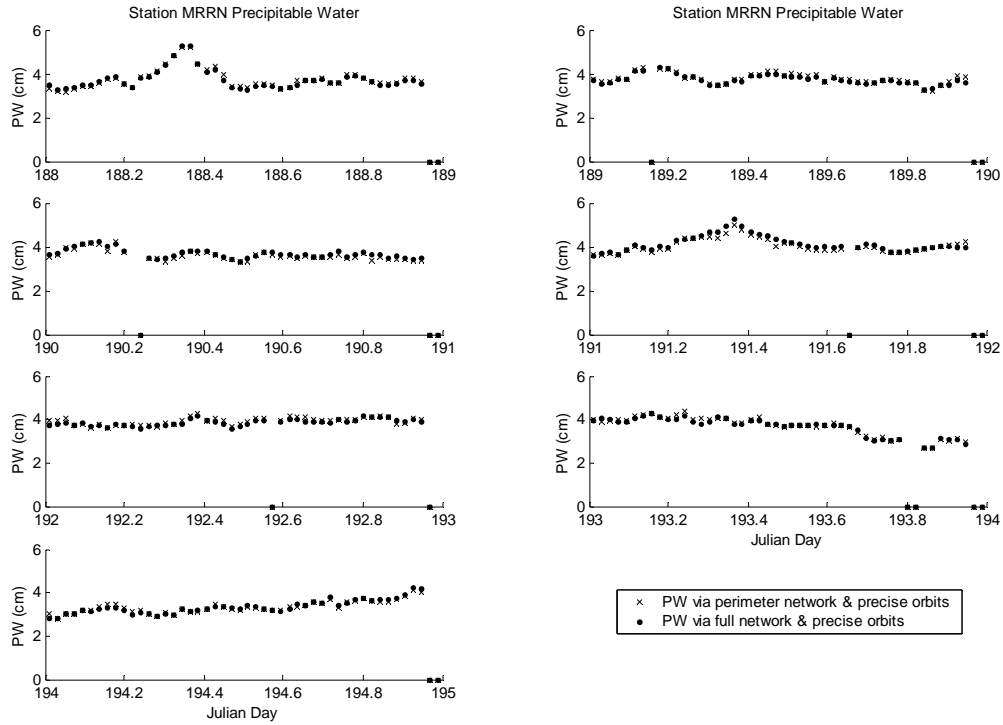
Figure 4-12. MRRN Degraded Network vs. Full Network PW Results

Notice the small relative errors and apparent minimal loss in the ability to estimate precipitable water. The error statistics for PW estimation under degraded network constraints (considering the full-network, precise orbit results as truth) are shown in Table 4-9.

Table 4-9. Degraded Network/Precise Orbits vs. Full Network/Precise Orbits PW Error Statistics (Degraded/Precise Results – Full /Precise Results)

Day	MEAN (cm)	STD (cm)	RMS (cm)
188	0.084537	0.10309	0.13319
189	0.044964	0.084475	0.095538
190	-0.088162	0.10190	0.13454
191	-0.061237	0.11907	0.13368
192	0.088410	0.10442	0.13667
193	0.028687	0.10232	0.10604
194	-0.012376	0.092126	0.092740
OVERALL	**0.018797**	**0.11978**	**0.12122**

4-17

The 0.2 mm mean indicates almost negligible bias to the degraded network PW estimation. Similarly, the 1.2 mm standard deviation and RMS shows a good data grouping and excellent overall accuracy. This shows a minimal loss in PW estimation accuracy at the station locations when the observation data and network geometry become more limited. However, this fails to give adequate insight into the ability to resolve the precipitable water in the perimeter network's central regions, which relies primarily upon interpolation of the water vapor field. Investigation into PW interpolation was accomplished, with results displayed in section 4.4.

4.3.3   Combination of Degradation Effects

To get a better understanding of how the two degradation effects impact PW estimation performance, less accurate orbits were applied to the perimeter network. By considering likely operational requirements for real-time estimation using limited network resources, this combination investigation gave more practical performance measurements. First, the degraded network was combined with the use of broadcast orbits. The extremely variant PW estimation seen previously with the use of broadcast orbits in the full network case gave a good indication of what was to be expected. Typical stations for the PW estimation with the perimeter network and broadcast orbits can be seen in Figures 4-13 and 4-14.
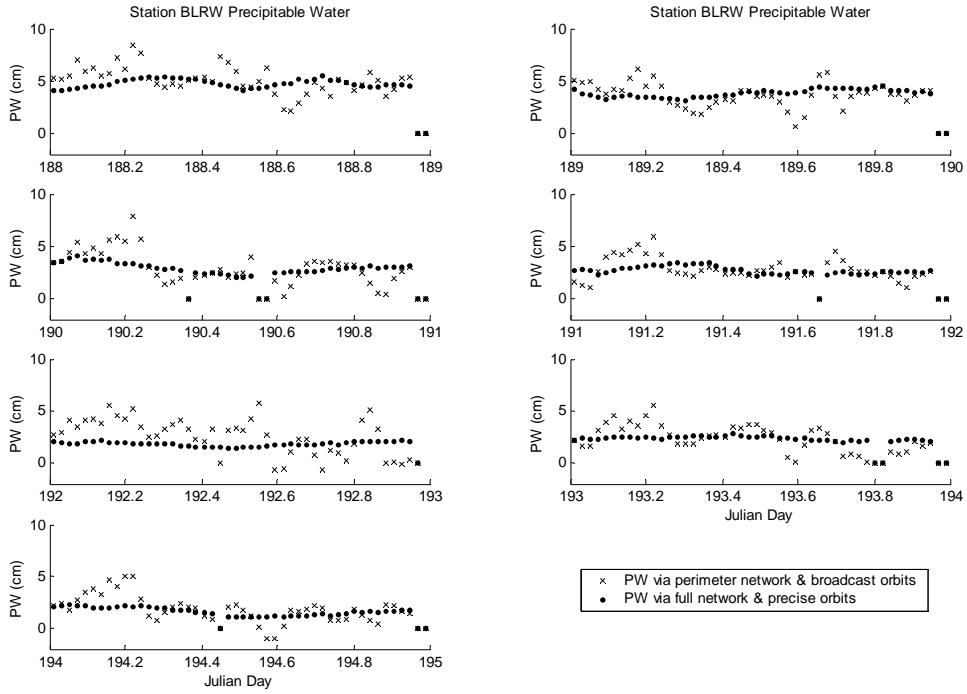
Figure 4-13. BLRW Degraded Network/Broadcast Orbits vs. Full Network/Precise Orbits PW Results
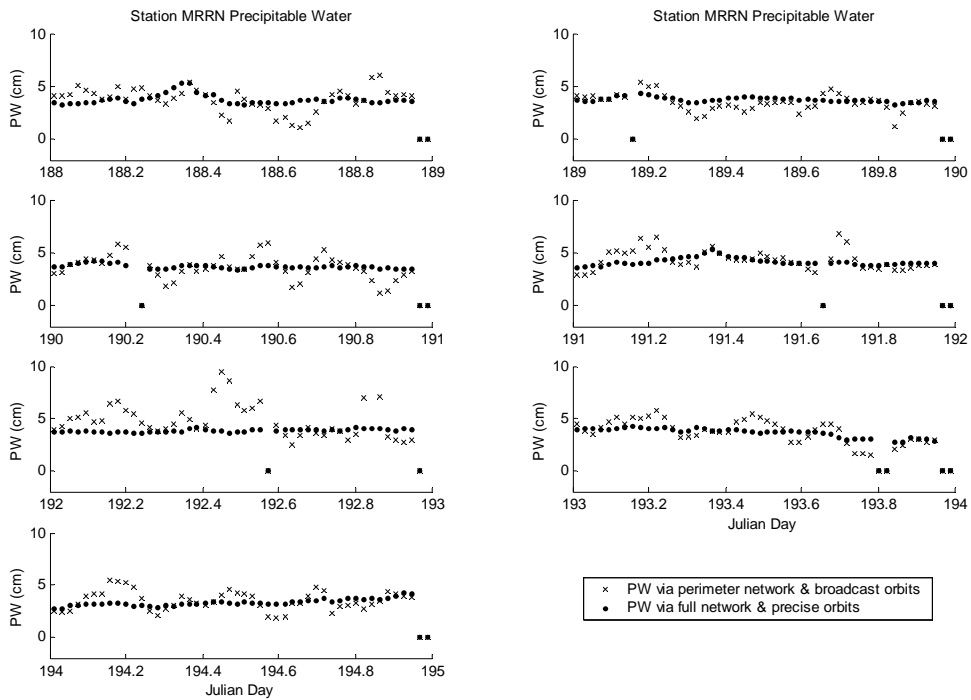
Figure 4-14. MRRN Degraded Network/Broadcast Orbits vs. Full Network/Precise Orbits PW Results

Again, it is evident that significant variation in precipitable water estimation is introduced by the gross inaccuracies present in the broadcast ephemeris, vastly outweighing the error introduced by a degenerated perimeter network. The error statistics for PW obtained from using broadcast orbits and the perimeter network (considering the full-network, precise orbit results as truth) are shown in Table 4-10.

Table 4-10. Degraded Network/Broadcast Orbits vs. Full Network/Precise Orbits PW Error Statistics (Degraded/Broadcast Results – Full/Precise Results)

Day	MEAN (cm)	STD (cm)	RMS (cm)
188	0.17169	1.3164	1.3255
189	-0.090260	0.95890	0.96110
190	0.078036	1.2704	1.2694
191	0.24578	0.92574	0.95600
192	1.0544	1.9060	2.1749
193	0.22347	1.0016	1.0240
194	0.16278	0.98925	1.003
OVERALL	**0.27479**	**1.2975**	**1.3259**

With a standard deviation and RMS of approximately 1.3 cm, the dominant error introduced by the broadcast orbits render PW estimation ineffective. The effects of broadcast orbit inaccuracies outweigh the degenerated network effects by an order of magnitude.

With the obvious requirement for a more accurate orbit, the ultra-rapid orbit was used in conjunction with the perimeter network. Knowing that previous analysis has indicated similar error magnitudes in both degradation sources, more realistic results were expected and observed. Typical stations for the PW estimation with the perimeter network and ultra-rapid orbits can be seen in Figures 4-15 and 4-16.
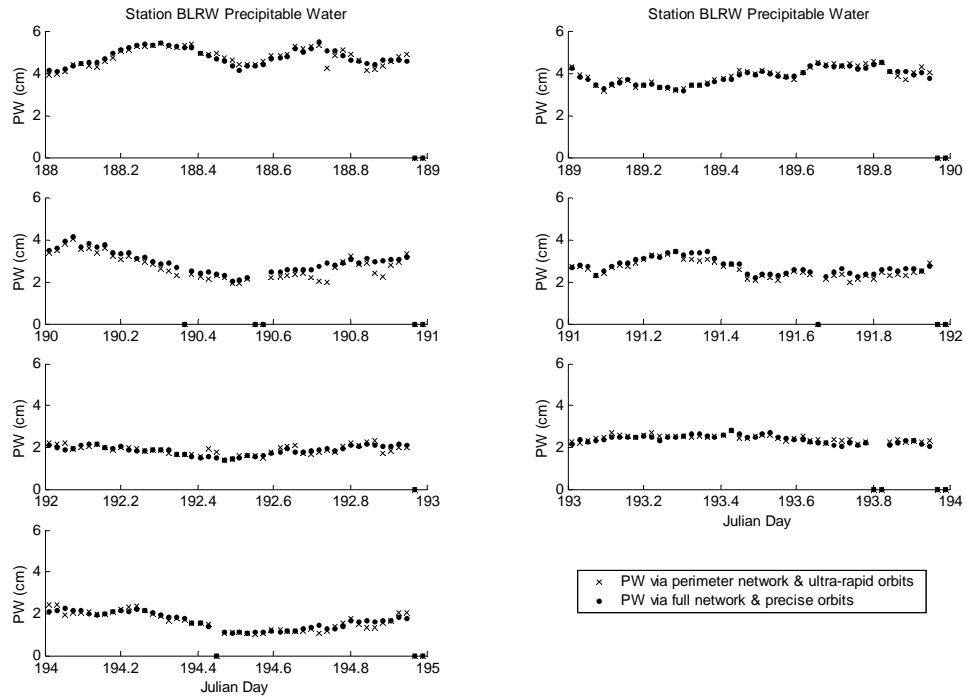
Figure 4-15. BLRW Degraded Network/Ultra-rapid Orbits vs. Full Network/Precise Orbits PW Results
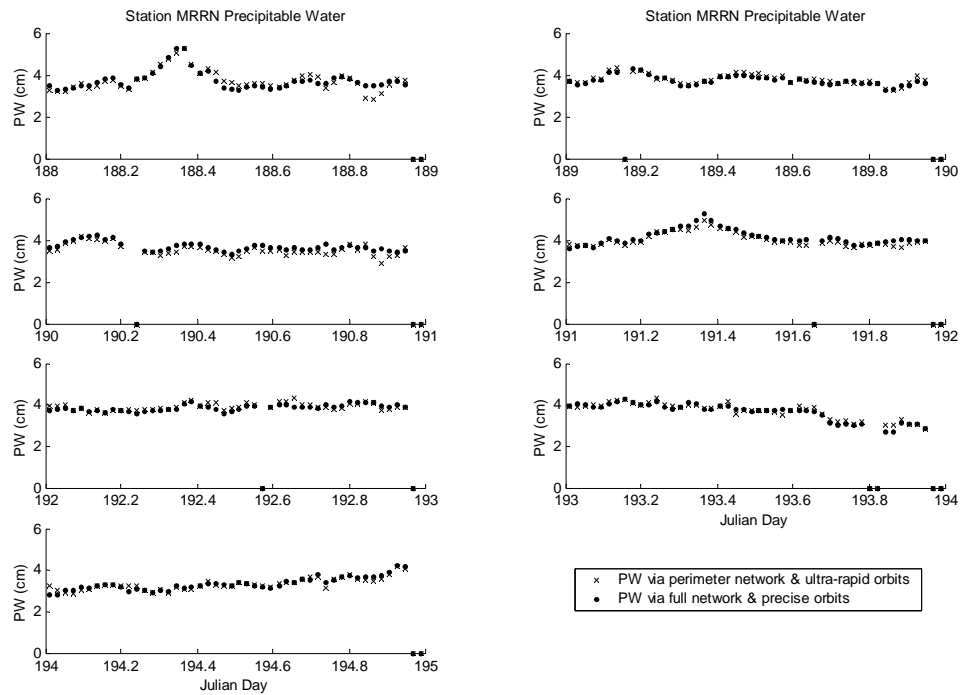
Figure 4-16. MRRN Degraded Network/Ultra-rapid Orbits vs. Full Network/Precise Orbits PW Results

Notice the consistently small relative errors and minimal compounding loss in the ability to estimate precipitable water. The error statistics for PW obtained from using ultra-rapid orbits and the perimeter network (considering the full-network, precise orbit results as truth) are shown in Table 4-11.

Table 4-11. Degraded Network/Ultra-rapid Orbits vs. Full Network/Precise Orbits PW Error Statistics (Degraded/Ultra-rapid – Full/Precise)

Day	MEAN (cm)	STD (cm)	RMS (cm)
188	0.048640	0.23405	0.23868
189	0.039705	0.098967	0.10644
190	-0.16201	0.17635	0.23912
191	-0.10491	0.13158	0.16808
192	0.071164	0.15792	0.17292
193	0.038411	0.13875	0.14366
194	0.0031923	0.14451	0.14420
OVERALL	**-0.0035491**	**0.18095**	**0.18093**

The results show an exceptional ability to estimate precipitable water despite the effects of the ultra-rapid orbit accuracy and degraded network. There is essentially no bias, and a 1.8 mm standard deviation and RMS indicate excellent overall accuracy. It appears that the need for real-time PW estimation is best suited by using ultra-rapid orbits, proven in all the investigated cases.

4.3.4   Ambiguity Resolution Discussion

It was initially perceived that the degraded network and the less accurate ephemerides would adversely affect the ability to resolve the carrier-phase ambiguities. The ambiguity resolution ability was examined by analyzing the Bernese output files. When the precise and ultra-rapid orbits were used, no difference in the resolution ability was observed, with an average of about 68 to 70 percent of the ambiguities regularly able

to be resolved. The consistency of the ambiguity resolution with both the precise and ultra-rapid orbits correlates strongly with the ability to accurately estimate precipitable water. The introduction of broadcast orbits provided significantly poorer ambiguity resolution with about 55 to 56 percent of the ambiguities to regularly be resolved. Moreover, several instances showed only 5 to 10 percent of the ambiguities were able to be resolved.

Further investigation was done to see how the degenerated perimeter network affected ambiguity resolution. A marginal decrease (1 to 2 percent) was observed when the precise and ultra-rapid orbits were implemented with the degraded network. However, the broadcast orbits used in conjunction with the degraded network displayed more significant resolution inability. Under this condition, only about 40 percent of the ambiguities were able to be regularly resolved. The poor ambiguity resolution associated with broadcast orbits provided another indicator of their inadequacy for determining precipitable water.

4.4 Interpolation Methods Investigation

Using the previous examination results, it was apparent that the ultra-rapid orbits used in conjunction with the degraded network was the most likely candidate for a military operations environment. Given the perimeter network utilizing ultra-rapid orbits, investigation was taken into how well the water vapor field over the region can be characterized when the precipitable water values are known at the perimeter stations. This required the use of an interpolation algorithm to find the intermediate PW values throughout the interior of the perimeter network. This thesis examines the adequacy of a

triangle-based linear and a triangle-based cubic interpolation scheme. Both interpolation

algorithms are MATLAB® functions, based on a Delaunay triangulation of the data. A

linear interpolation best fits a planar surface to the data, whereas a cubic interpolation

will best fit a smoother, curved surface [7].

4.4.1 Triangle-based Linear Interpolation

The first scenario to be investigated was the triangle-based linear interpolation

scheme in conjunction with degraded perimeter network and ultra-rapid orbits. Because

of the triangle-based interpolation schemes in both examined methods, only the points

that lie within the perimeter network are able to be resolved. As a result, station HKLO

cannot be interpolated because of its outlying position near the PRCO/CNWM baseline.

Figure 4-17 displays the graphical results of the linear interpolation method applied over

the region. The left plot is the perimeter network with the PW interpolation applied over

the region. The right plot represents the truest known representation of the water vapor

field, using the full 18-station network to interpolate over the region.
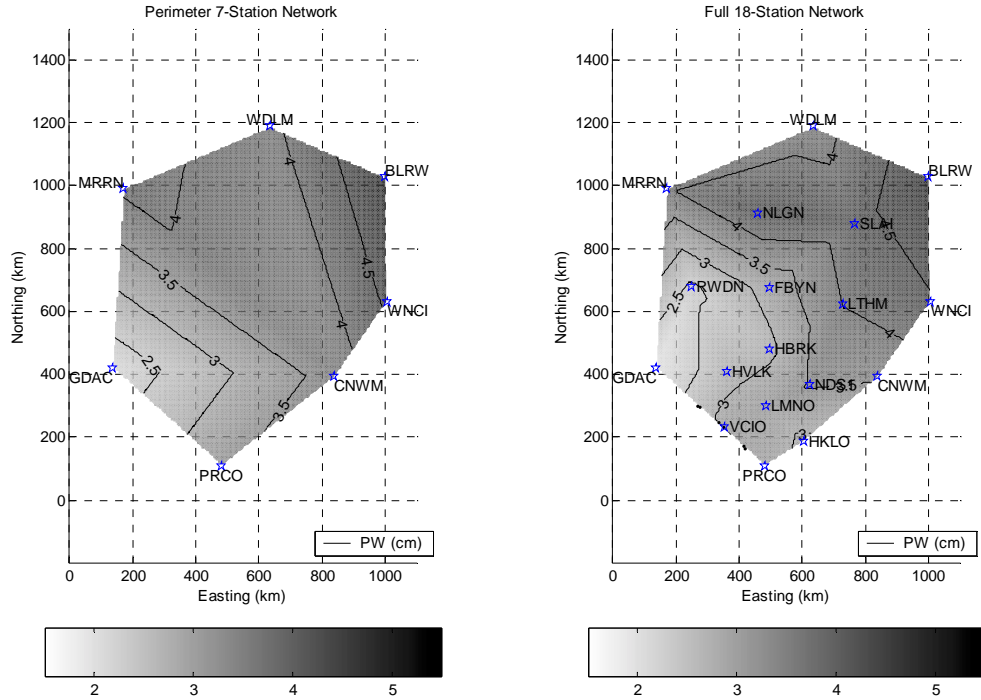
Figure 4-17. Perimeter Network vs. Full Network Linear Interpolation

It should be noted that interpolation accuracy is dependent upon station location relative to the known data on which the interpolation is based. As a result, only minimal information can be gained from an overall statistical view. This can be seen in Figure 4-17, as the resolution in the central areas show significant differences with missing observed data points.   To properly characterize interpolation performance the statistics are calculated by station location, knowing that stations furthest away from all known data points should have the poorest interpolation. The perimeter network linear interpolation statistics are shown in Table 4-12.

**Table 4-12. Linear Interpolation Error Statistics With Isolated Stations Highlighted
(Interpolated Results – Estimated Results)**

STATION	MEAN (cm)	STD (cm)	RMS (cm)
BLRW	0.097608	0.16523	0.18980
CNWM	0.17107	0.19276	0.25559
FBYN	0.36562	0.45191	0.57611
GDAC	0.098485	0.23093	0.24791
HBRK	0.12044	0.30962	0.32795
HKLO	N/A	N/A	N/A
HVLK	-0.10752	0.19056	0.21635
LMNO	-0.15889	0.13825	0.20872
LTHM	-0.17528	0.19316	0.25872
MRRN	0.082085	0.21431	0.22653
NDS1	0.050782	0.27626	0.27687
NLGN	-0.44182	0.51602	0.67336
PRCO	0.12171	0.30368	0.32299
RWDN	0.73933	0.35051	0.81570
SLAI	-0.48279	0.49795	0.68797
VCIO	-0.094812	0.25679	0.27017
WDLM	0.10724	0.16852	0.19765
WNCI	0.13227	0.18020	0.22139
OVERALL	**0.03798**	**0.39647**	**0.39793**

The highlighted stations are those located in the interpolated perimeter network's central-most regions. These are observed to have the worst PW estimation statistics as expected, as they are the hardest values to actually interpolate. Notice how the RMS errors all exceed 0.5 cm, indicative of a fairly variant PW interpolation at these station locations. A graphical depiction of the RMS error over the network region is shown in Figure 4-18. The RMS error peaks encompassing stations RWDN, NLGN, and SLAI show the increased errors present in network areas lacking PW data.
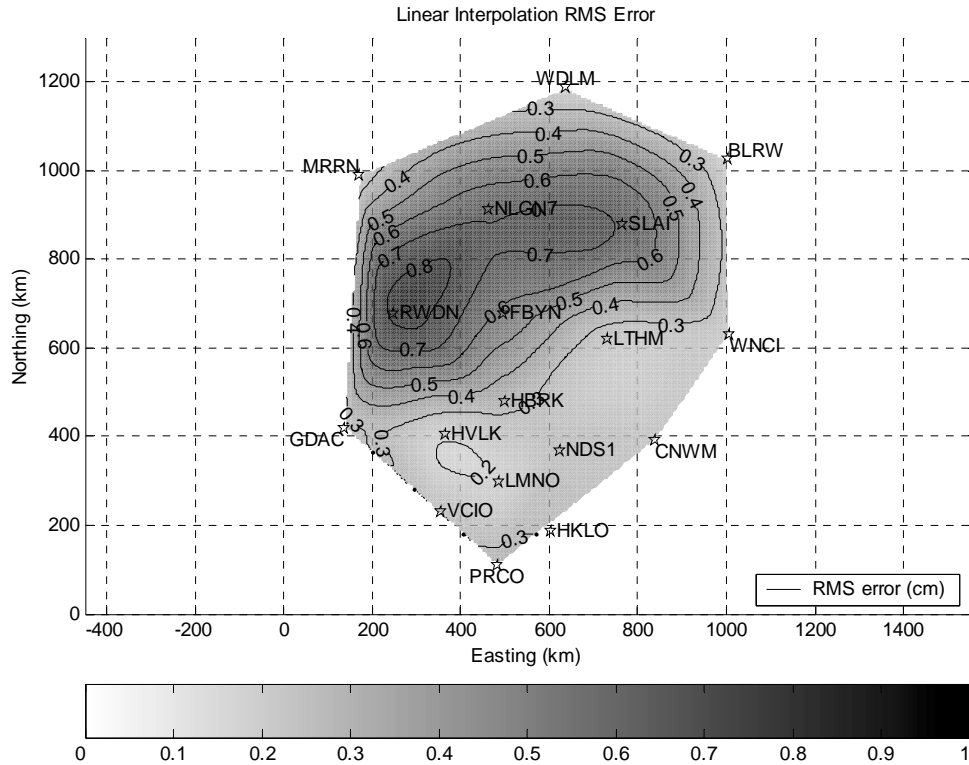
Figure 4-18. Linear Interpolation RMS Error Over Network Region

The perimeter stations (BLRW, CNWM, GDAC, MRRN, PRCO, WNCI, and WDLM) suspiciously have interpolation error, even though the interpolation was based on the data at those locations. This results from comparing the perimeter interpolation with the full-network PW solution. Recall that the estimated PW values at the stations in the degraded perimeter network varied slightly from the full-network PW estimations at those same locations. In effect, we are seeing the combined error effects of degraded network PW estimation and network interpolation.

4.4.2   Triangle-based Cubic Interpolation

The second investigation used the triangle-based cubic interpolation scheme in conjunction with degraded perimeter network and ultra-rapid orbits. The cubic interpolation scheme should experience similar problems with the perimeter network's central-most regions, as it utilizes the same basic interpolation strategy. Figure 4-19 displays the graphical results from using the cubic interpolation method applied over the region, with the same subplots as described previously.
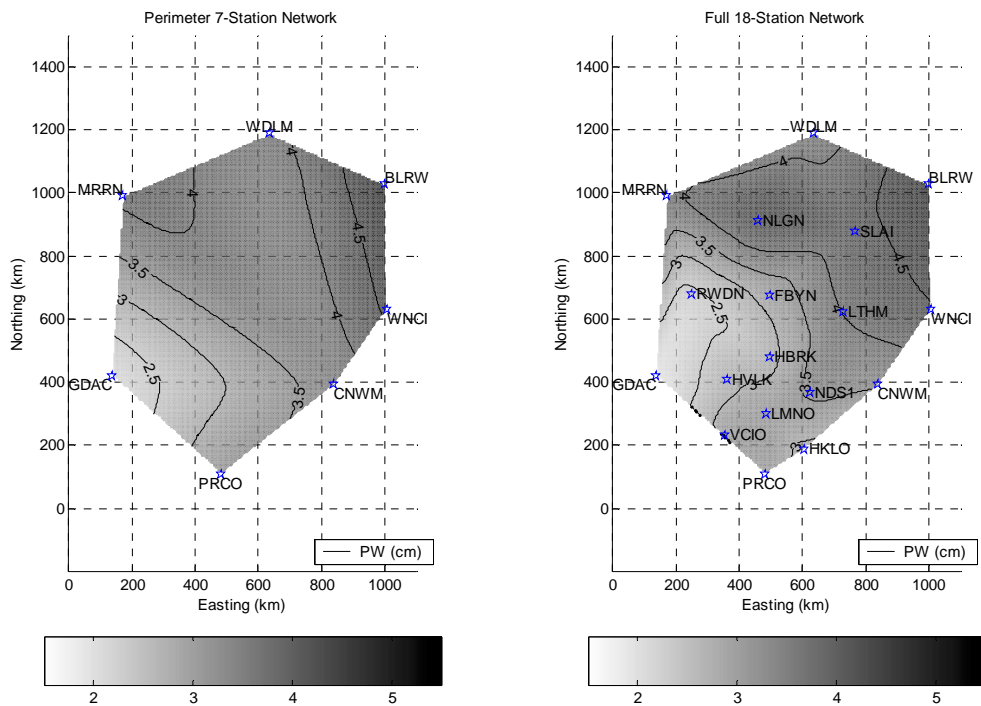
Figure 4-19. Perimeter Network vs. Full Network Cubic Interpolation

Very little difference is present between the linear interpolation in Figure 4-17 and the cubic interpolation in Figure 4-19. Essentially the cubic interpolation provides a smoother fit to the interpolated data throughout the network, more consistent with how the water vapor field typically is distributed. The perimeter network cubic interpolation statistics are shown in Table 4-13, again with the central-most stations highlighted.

**Table 4-13. Cubic Interpolation Error Statistics With Isolated Stations Highlighted
(Interpolated Results – Estimated Results)**

STATION	MEAN (cm)	STD (cm)	RMS (cm)
BLRW	0.097608	0.16523	0.18980
CNWM	0.17107	0.19276	0.25559
FBYN	0.27606	0.46463	0.53455
GDAC	0.098485	0.23093	0.24791
HBRK	0.062910	0.33032	0.33146
HKLO	N/A	N/A	N/A
HVLK	-0.11039	0.18708	0.21484
LMNO	-0.20210	0.13435	0.24113
LTHM	-0.21440	0.19649	0.28886
MRRN	0.082085	0.21431	0.22653
NDS1	0.012016	0.29056	0.28651
NLGN	-0.47032	0.52242	0.69703
PRCO	0.12171	0.30368	0.32299
RWDN	0.68891	0.36229	0.77555
SLAI	-0.51374	0.50823	0.71705
VCIO	-0.16861	0.25206	0.30015
WNCI	0.10724	0.16852	0.19765
WDLM	0.13227	0.18020	0.22139
OVERALL	**0.011712**	**0.39951**	**0.39933**

A graphical depiction of the cubic interpolation RMS error over the network region is

shown in Figure 4-20. Again, the RMS error peaks encompassing stations RWDN,

NLGN, and SLAI show the increased errors present in network areas lacking PW data.
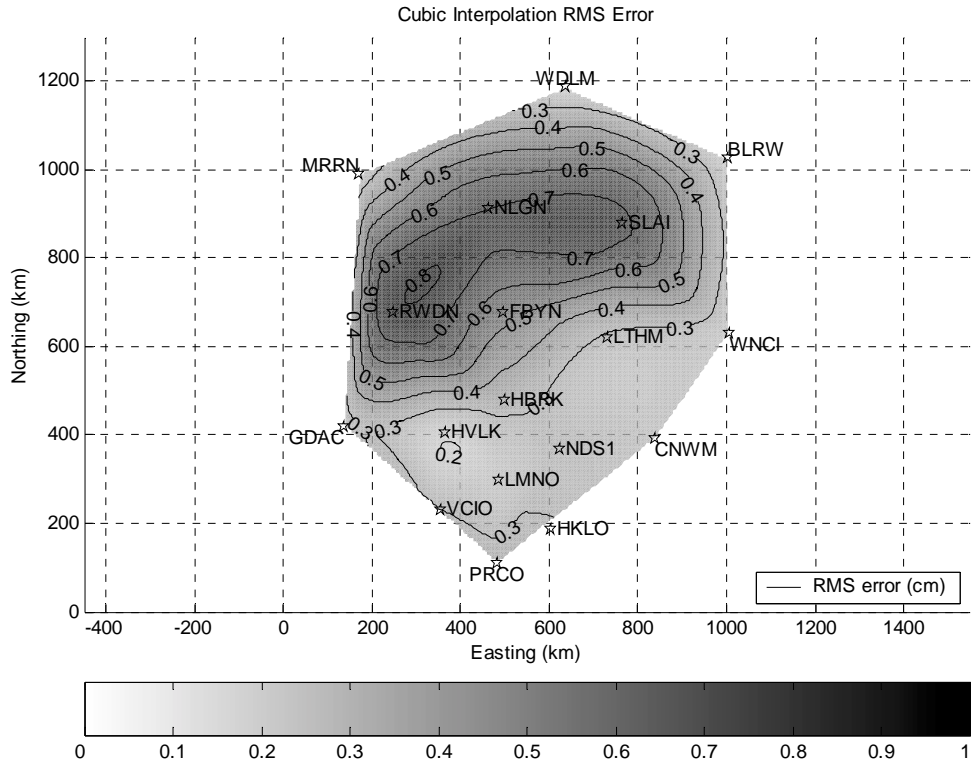
Figure 4-20. Cubic Interpolation RMS Error Over Network Region

There is very little statistical difference between the linear and cubic interpolation schemes, as the cubic interpolation is still consistent RMS errors in excess of 0.5 cm at the highlighted central stations. However, these highlighted stations are all worse for the cubic case by a small amount (~ 0.2 to 0.4 mm). As in the linear interpolation case, the perimeter stations (BLRW, CNWM, GDAC, MRRN, PRCO, WNCI, and WDLM) do not have zero error as a result from comparing the perimeter interpolation to the full-network PW solution. It initially appears that the stand-alone ability to interpolate using these basic schemes may be inadequate for effective PW determination.

4.4.3 Alternate Perimeter PW Data Investigation

In the first two interpolation investigations, the perimeter network PW values were used to interpolate the PW throughout the region, and then the interpolation was compared to the full-network solution at each station location. This has an inherent flaw from comparing different known perimeter values, as the estimation of PW for the perimeter network produced slightly different results from the full-network estimation of PW. Ideally, there should be no PW interpolation error for the 7 perimeter stations, thereby seeing the error impact of the interpolation method alone. Using the data from the 7 stations along the full-network perimeter solution, another cubic interpolation was done to observe the impact of the interpolation scheme by itself. The differences between the two different interpolation sets are shown in Figure 4-21.
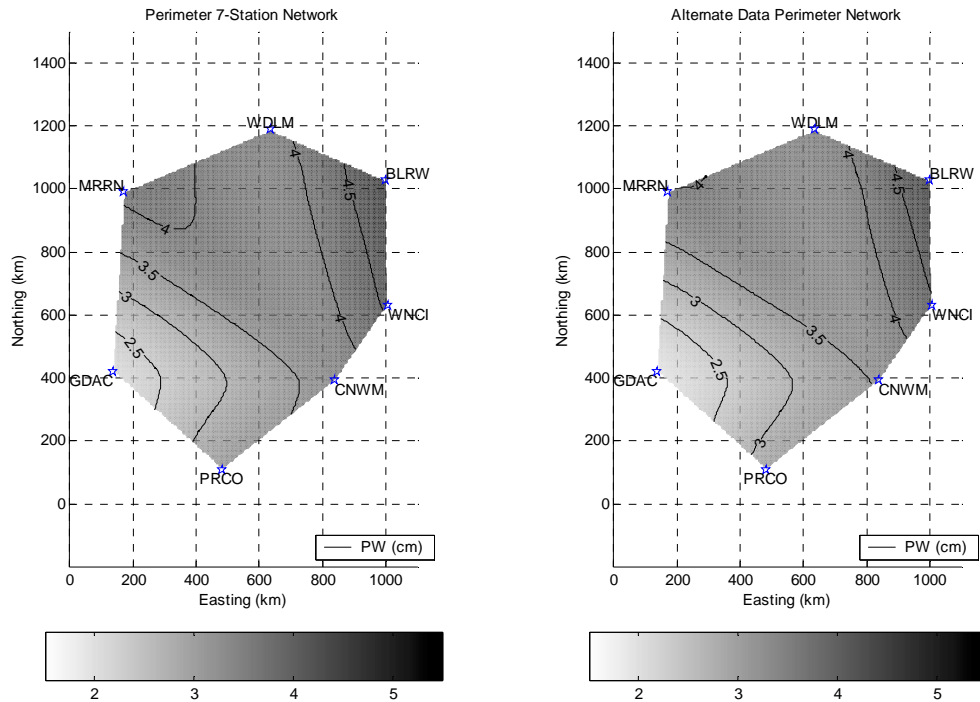
Figure 4-21. Perimeter Network Interpolation vs. Perimeter Network Interpolation (Using Full Network Data)

Although the impact does not appear to be drastic, there is a noticeable difference in the

interpolated PW over the network region. The alternate data perimeter network is

compared to the full-network solution in Figure 4-22.
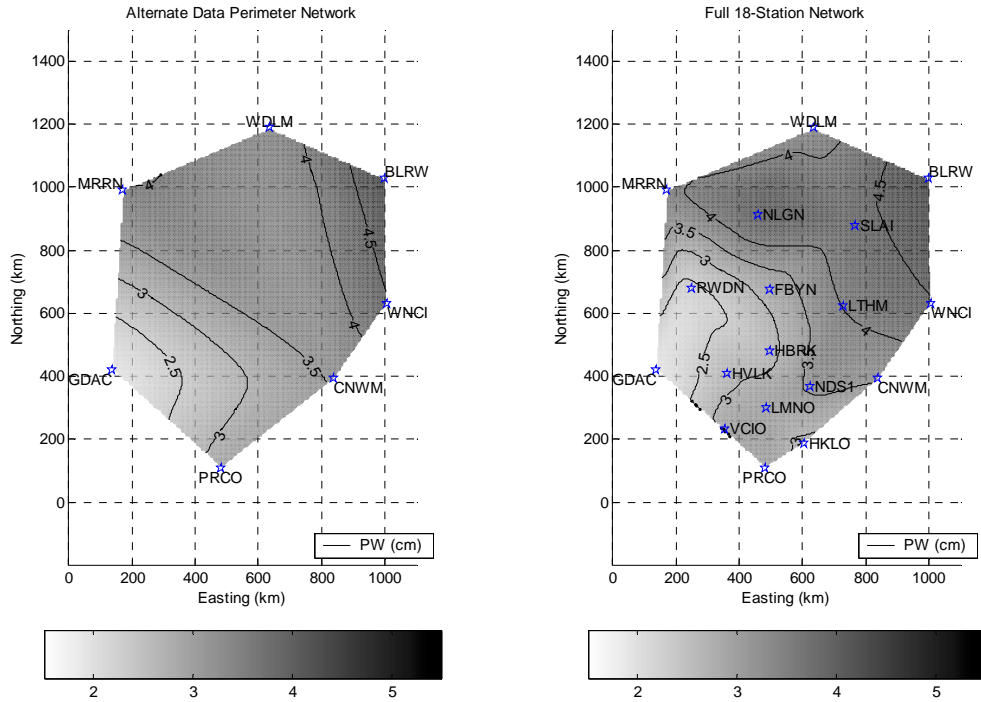
Figure 4-22. Perimeter Network Interpolation (Using Full Network Data) vs. Full Network Interpolation

Notice how the alternate data interpolation still fails to provide a good PW

characterization throughout the entire network region. The alternate data perimeter

network statistics are shown in Table 4-14, with the same central stations highlighted.

The perimeter stations all have error statistics equal to zero, as the perimeter station PW

data now matches the full-network data.

**Table 4-14. Perimeter Network Interpolation (Using Full Network Data)
Error Statistics With Isolated Stations Highlighted
(Interpolated Results – Estimated Results)**

STATION	MEAN (cm)	STD (cm)	RMS (cm)
BLRW	0	0	0
CNWM	0	0	0
FBYN	0.14688	0.35929	0.38323
GDAC	0	0	0
HBRK	-0.074209	0.18630	0.19797
HKLO	N/A	N/A	N/A
HVLK	-0.23423	0.17679	0.29189
LMNO	-0.39427	0.13210	0.41494
LTHM	-0.36657	0.14165	0.39224
MRRN	0	0	0
NDS1	-0.14040	0.32727	0.35166
NLGN	-0.58116	0.47265	0.74457
PRCO	0	0	0
RWDN	0.56743	0.27880	0.63017
SLAI	-0.64019	0.38907	0.74598
VCIO	-0.28345	0.27661	0.39320
WNCI	0	0	0
WDLM	0	0	0
OVERALL	**-0.11492**	**0.35014**	**0.36822**

The errors have slightly decreased, with the highlighted stations now showing the poorest performance with RMS errors in excess of 0.6 cm. The performance at stations NLGN and SLAI actually increased in RMS error, while RWDN showed a minimal decrease in RMS error. The inconsistent improvement in error statistics indicates the dominant effect of the interpolation error. Figure 4-23 graphically shows the comparison of RMS error over the network region. The RMS error from the original perimeter network PW data interpolation is shown on the left plot, and the RMS error from the alternate full network perimeter PW data interpolation on the right.
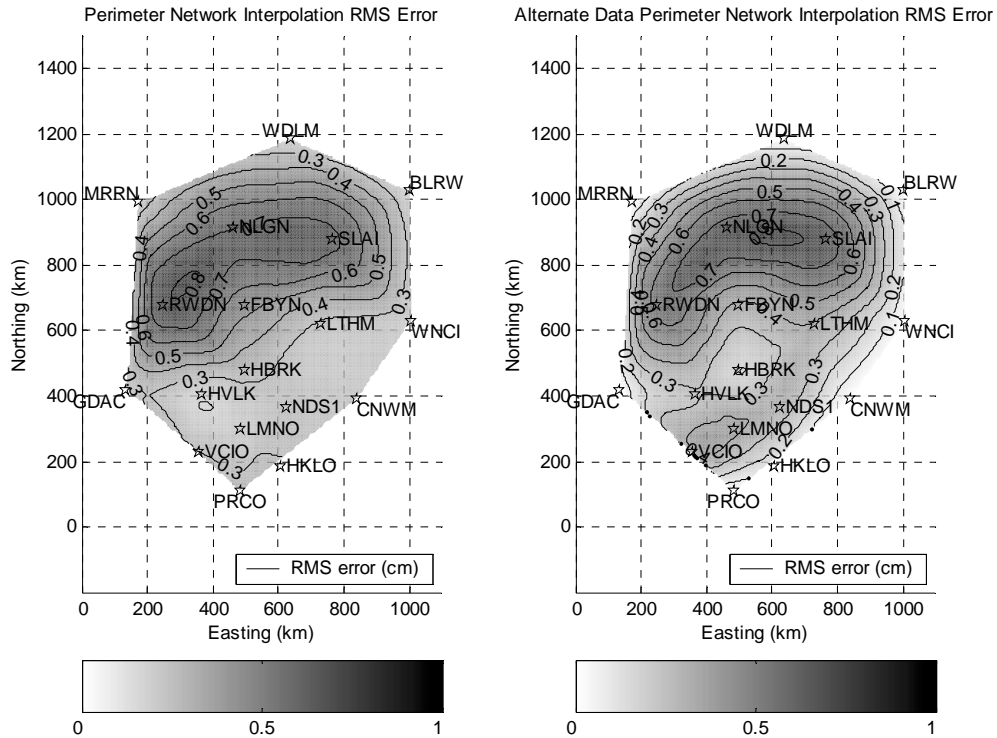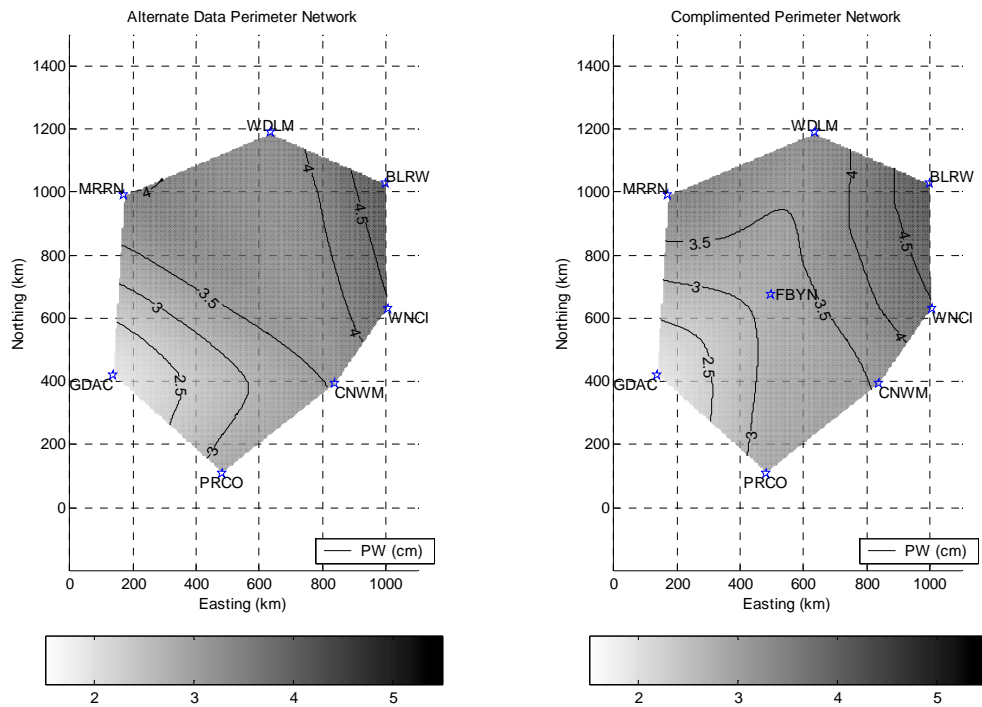
Figure 4-23. Perimeter Network Interpolation RMS Error vs. Perimeter Network Interpolation (Using Full Network Data) RMS Error

Notice the minimal RMS error difference between the different perimeter PW data interpolation cases. A strong RMS error peak is present around the stations RWDN, NLGN, and SLAI in both scenarios, with a small offset between them. Again, this shows the dominant interpolation error effect.

4.4.4   Complimented Network Investigation

With the obvious accuracy restriction imposed by the interpolation schemes, adding a station in the network's center was investigated. To accomplish this, PW data from the full network solution for the stations BLRW, CNWM, FBYN, GDAC, MRRN, PRCO, WNCI, and WDLM was used to form the complimented network. This would help compensate for the shortcoming of the interpolation algorithms by providing an

additional data source in a much-required part of the network. Additionally, this would

be a distinct capability in a remote military operating environment. Increased ability to

interpolate PW values throughout the network region was expected and observed, as

Figure 4-24 shows the relative increase in resolution.

**Figure 4-24. Perimeter Network Interpolation vs. Complimented
Network Interpolation (Both Using Full Network Data)**

The interpolation difference associated with the complimented network is readily

noticeable. The relative improvement is shown in Figure 4-25, with comparison to the

full-network solution.
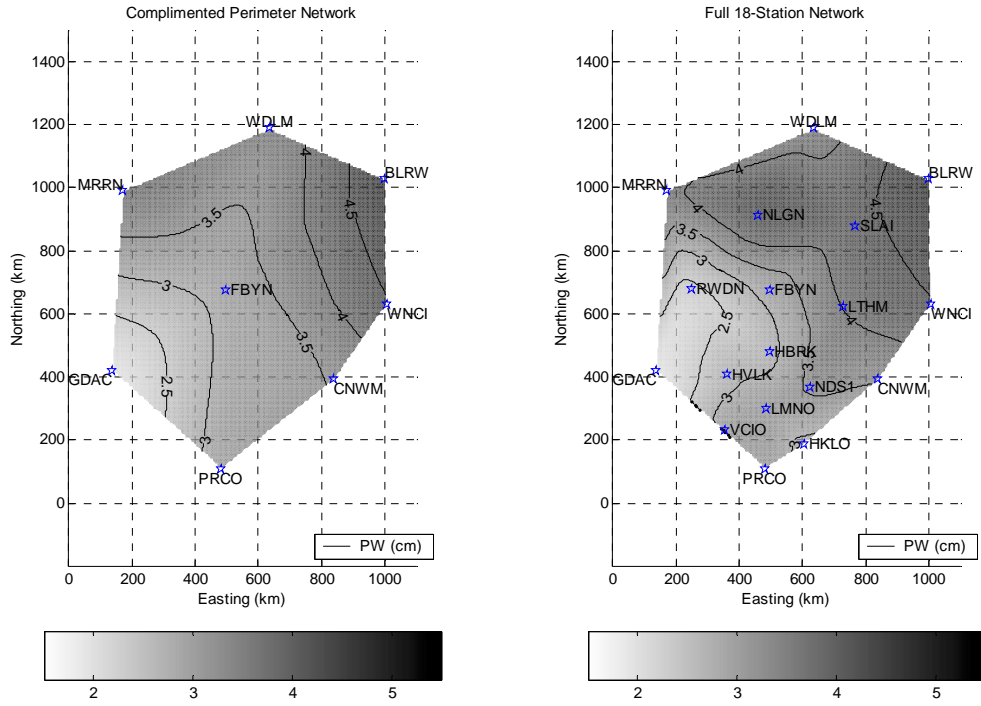
Figure 4-25. Complimented Network Interpolation (Using Full Network Data) vs. Full Network Interpolation

Despite the changed PW interpolation over the region via the complemented network, it still falls short compared to the full-network solution. The statistics for the complimented network error performance are shown in Table 4-15.

Table 4-15. Complimented Network Interpolation Error Statistics With Isolated Stations Highlighted (Interpolated Results – Estimated Results)

STATION	MEAN (cm)	STD (cm)	RMS (cm)
BLRW	0	0	0
CNWM	0	0	0
FBYN	0	0	0
GDAC	0	0	0
HBRK	0.22331	0.13739	0.26113
HKLO	N/A	N/A	N/A
HVLK	0.055507	0.29500	0.29588
LMNO	-0.10388	0.19259	0.21526
LTHM	-0.027974	0.37173	0.36729
MRRN	0	0	0
NDS1	0.11973	0.36231	0.37649
NLGN	-0.71832	0.38604	0.81271
PRCO	0	0	0
RWDN	-0.47471	0.19638	0.51248
SLAI	-0.38724	0.23583	0.45147
VCIO	-0.19013	0.31178	0.36124
WNCI	0	0	0
WDLM	0	0	0
OVERALL	**-0.032464**	**0.31582**	**0.31721**

The largest variations are still encountered at station NLGN, with an RMS error exceeding 0.8 cm. Stations RWDN and SLAI had a noticeable improvement, lowering their RMS errors to just over 0.51 and 0.45 cm, respectively. Figure 4-26 graphically shows the comparison of RMS error over the network region. The RMS error resulting from the perimeter network PW data interpolation is shown on the left plot, and the RMS error from the complimented network PW data interpolation on the right.
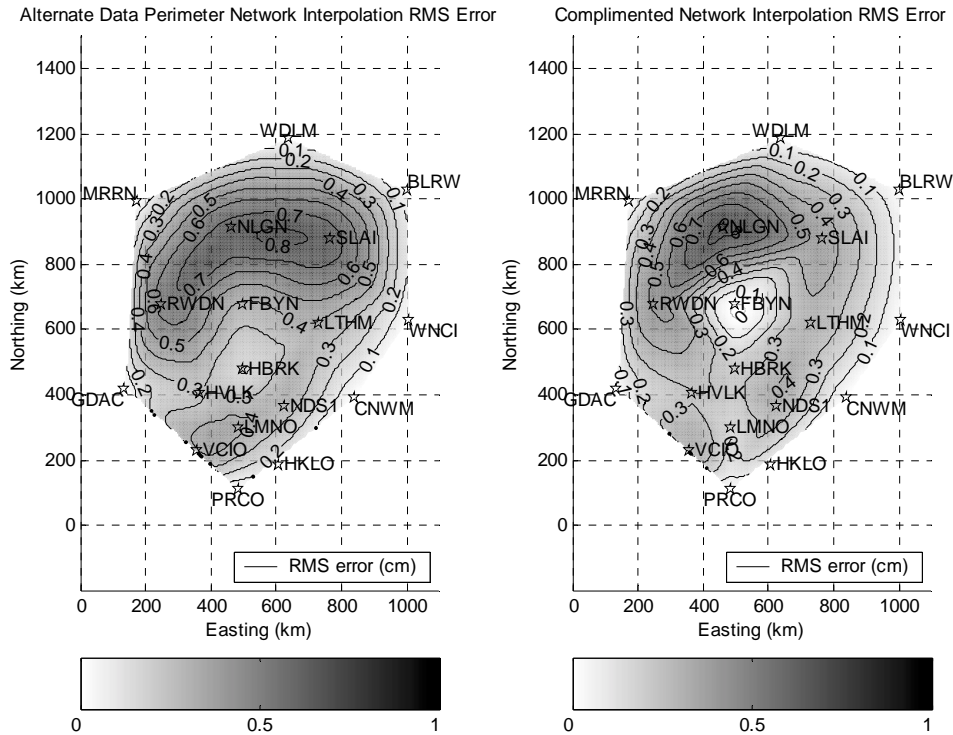
Figure 4-26. Perimeter Network Interpolation RMS Error vs. Complimented Network Interpolation RMS Error (Both Using Full Network Data)

Notice the RMS error difference between the two interpolation cases. A strong RMS error peak is present around the stations RWDN, NLGN, and SLAI in both scenarios, but with a decreased effect in the complimented network case. The peak area shrinks while maintaining its amplitude due to the known PW data present at station FBYN. This shows how the interpolation of PW is only good around known data points, and deteriorates rapidly as distance from the data increases. The complimented network showed an improvement, but did not eliminate the RMS error in excess of 0.8 cm in the worst areas of the network. It appears that complimenting the network with a centrally located data source will slightly enhance the determination of the PW over the network region; however, interpolation schemes do have significant accuracy limitations due to the random nature of PW distributions over the region.

4.4.5 Sequential Time Investigation

In an attempt to provide a better depiction showing PW interpolation over the network region progresses with time, a typical period of 2 hours consecutive hours was investigated. A complimented network interpolation was done at 0, 1, and 2 hour time epochs, with the corresponding full-network solution also displayed. This would provide additional insight into how the progressive interpolations actually compare to the best-estimated activity in the network region during this time period. Figures 4-27, 4-28, and 4-29 show the hourly epochs over the two-hour window.
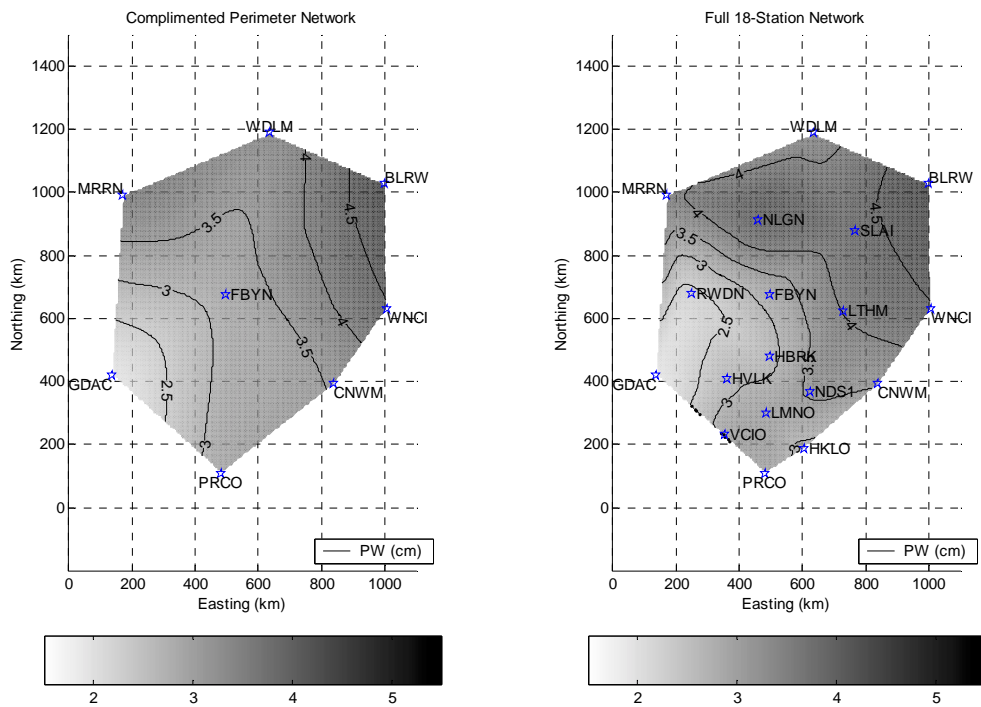
Figure 4-27. Hour 0 Complimented Network Interpolation (Using Full Network Data) vs. Full Network Interpolation
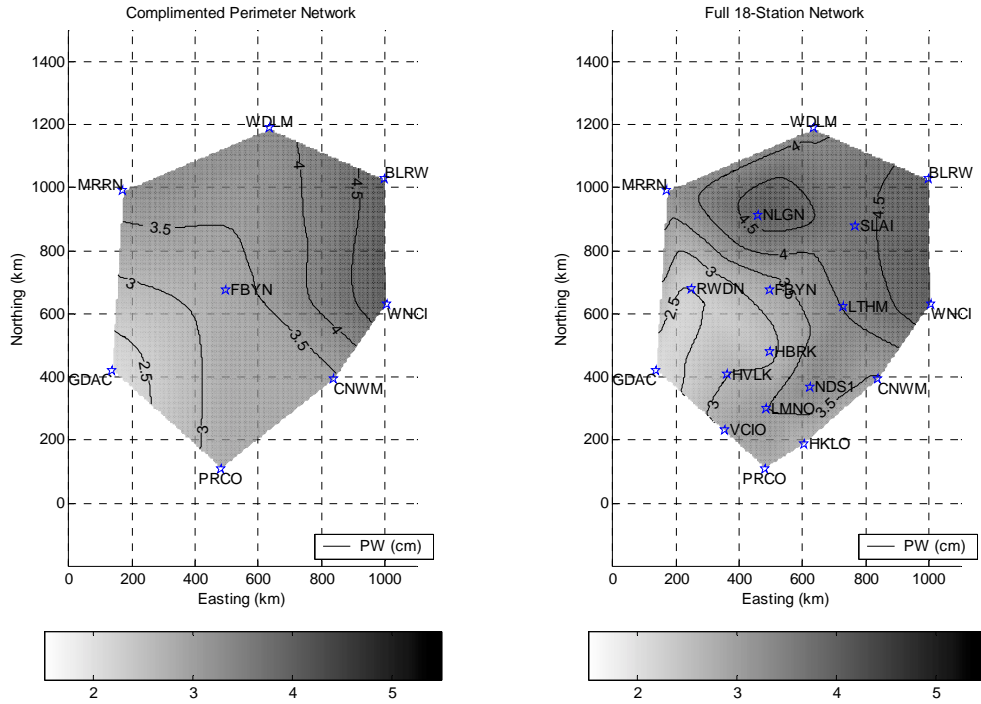
Figure 4-28. Hour 1 Complimented Network Interpolation (Using Full Network Data) vs. Full Network Interpolation
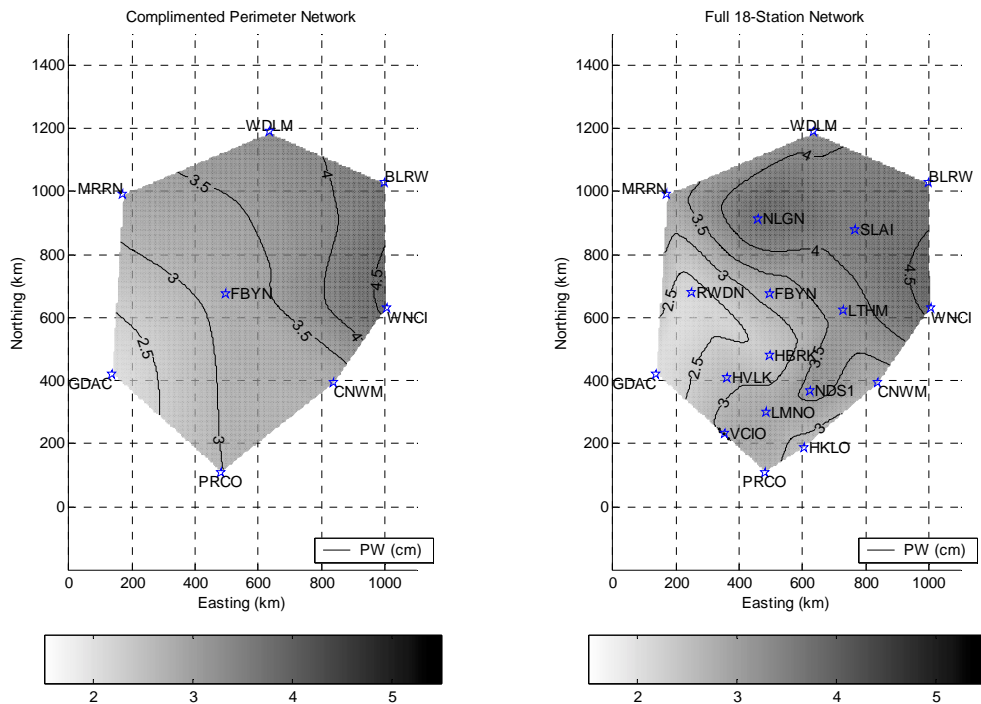
Figure 4-29. Hour 2 Complimented Network Interpolation (Using Full Network Data) vs. Full Network Interpolation

Notice how the PW around NLGN changes significantly over this 2-hour window. The interpolation is unable to resolve the peak that forms at station NLGN, unless a data source is present. Furthermore, the changes appear to be more gradual in the interpolated progression, whereas the full-network solution shows a more drastic change in the PW distribution. It appears that the water vapor field shape and distribution contributes more significantly than the distance an interpolated point is from the surrounding data sources.

4.5 Summary

This chapter presented the performance results of GPS-based precipitable water determination methods. Three main phases of investigation were accomplished: Process initialization, degradation effects, and interpolation ability. Substantial insight into the factors affecting the estimation of precipitable water was gained through these investigation steps. Both independent and coupled effects were observed and quantified by graphical and statistical methods.

Process initialization involved station coordinate estimation and methodology validation. Coordinates were estimated with the 7 days of data and were compared with each daily coordinate solution and the ITRF97 NGS coordinate solution. Good, consistent results (~ 2 to 4 cm) were obtained after elimination of initial network offsets. A tighter coordinate solution could have been generated using a longer data set. The methodology validation revealed excellent PW results in comparison to the NOAA GPS-MET derived PW values. A small bias (~ 2 mm) was consistently present, and a very tight precipitable water data set resulted from the algorithms employed by this thesis.

In the degradation investigation, decreased accuracy ephemerides and restricted network geometry and data sources were evaluated. The gross inaccuracy of the broadcast orbit rendered it virtually unusable for PW estimation purposes. However, the IGS ultra-rapid orbit showed a minimal loss (~ 1 to 2 mm) in PW estimation ability when compared to precise orbit derived results. Network geometry and data availability limitations showed minimal effects (~ 1 to 2 mm) on PW estimation ability. Moreover, the degraded perimeter network used in conjunction with ultra-rapid orbits demonstrated a good ability to estimate PW at the perimeter locations, with results on the order of about 3 to 4 mm. This showed promise for potential military operational considerations.

Finally, the ability to interpolate the precipitable water over the network region was investigated. Both triangle-based linear and triangle-based cubic interpolation schemes were implemented, and showed nearly identical statistics. Neither of these interpolation schemes independently provided accurate PW determination across the network region, with RMS errors in the most isolated locations exceeding 0.7 to 0.8 cm. Complimenting the degraded perimeter network with a central data source was done to see if the interpolation could be significantly improved. However, even the complimented network was not very successful in presenting a result with an accurate resolution, with isolated locations maintaining RMS errors exceeding 0.5 to 0.8 cm. This highlighted the inaccuracy of the linear and cubic interpolation algorithms, except for locations in close proximity to the known data points.

V. Conclusions and Recommendations

5.1 Overview

This research presented the theory, methodology, and results from using a GPS-based process for atmospheric precipitable water determination. Past research has indicated that increased atmospheric resolution and monitoring is a valuable asset for passive GPS-based methods, which can further compliment existing meteorological data sources. Further research has also developed mathematical algorithms for calculating precipitable water, using atmospheric constants, measurements, and models. This research did not seek to develop new algorithms, but rather analyzed the robustness and accuracy potential of existing algorithms in a military context.

Several investigations were done to characterize the GPS PW estimation performance under different constraints. First, GPS ephemeris degradation was performed to observe how decreased accuracy real-time orbits affected PW estimation. This investigation mainly dealt with the near real-time requirement for effective use of the data. Secondly, network degradation was implemented to quantify the effects that limited data availability and network geometry have on PW estimation. This investigation primarily dealt with the military restrictions that may be imposed on the network in remote operating locations. Finally, interpolation methods were applied to the degraded network using IGS ultra-rapid orbits to examine potential PW estimation ability given military operational restrictions. Interpolation method applications examined how

well the water vapor field can be characterized over the region given different available

PW data sets.

5.2 Conclusions

The GPS precipitable water algorithm and thesis methodology initially performed extremely well. During initial validation, PW estimates from the full 18-station network using precise orbits compared closely (~ 1 to 2 millimeters) with the NOAA GPS-MET PW estimates. The NOAA data was used as a basis of comparison, because no absolute truth source was available. The small relative errors between PW estimates demonstrated the consistency of the GPS PW algorithm with other independent sources.

The degradation investigations provided good insight into the factors affecting GPS PW determination. The overall results are depicted in Figure 5-1.
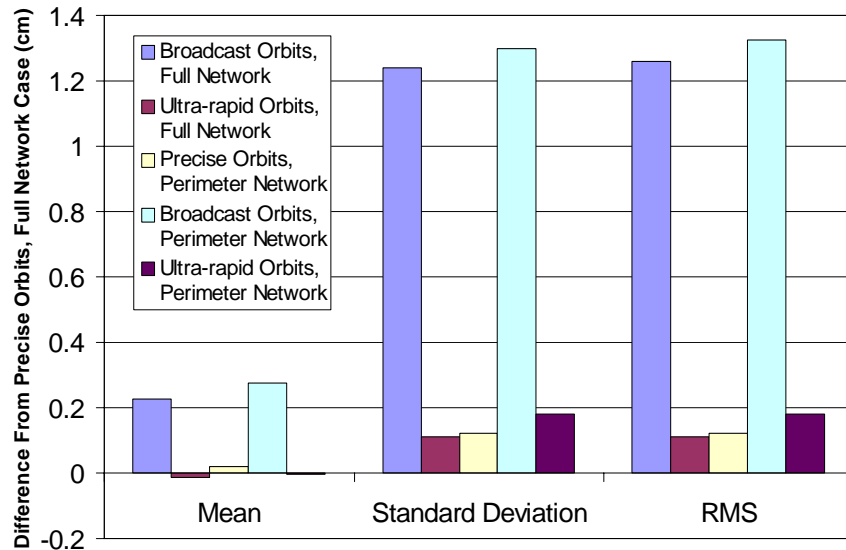
Figure 5-1. Degradation Investigation Summary

The orbit degradation investigation showed inadequacy of the broadcast ephemeris to facilitate PW estimation. The limiting factor appeared to be the inaccuracy present in

these orbits, causing PW RMS estimation errors exceeding 1 centimeter. A significant improvement was found in the IGS ultra-rapid orbits. These near real-time orbits showed minimal loss in the ability to estimate PW, with RMS errors on the order of 1 millimeter. As a result, they are the most likely candidates for real-time GPS PW estimation applications. It appears that orbit accuracy directly contributes to the ability to estimate PW, as an order of magnitude of improvement was seen in both the orbit accuracy and PW estimation error when moving from broadcast to ultra-rapid orbits.

Investigation into network degradation showed minimal impact on PW estimation at the included network stations. The network degradation to 7 perimeter stations introduced RMS errors of about 1 millimeter, with good overall performance. Introduction of less accurate orbits in conjunction with the 7-station perimeter network yielded similar effects to the previous investigation of degraded orbits. The broadcast ephemeris introduced PW estimation errors that vastly outweigh the effects of network degradation, again with RMS errors exceeding 1 centimeter in this combined case. This reaffirmed the inadequacy in using broadcast orbits for PW estimation. The ultra-rapid orbits in conjunction with the network degradation showed good performance, with RMS errors on the order of 2 millimeters. This smaller error is consistent with the performance of both the network and orbit degradations together. Through this investigation, the degraded perimeter network used in conjunction with ultra-rapid orbits is the best candidate for near real-time operational constraints.

Another important factor was the ability for the Bernese software to resolve the ambiguities given both the introduction of the orbit inaccuracies and limited data

availability. The ability for the Bernese software to resolve ambiguities given the different degradation combinations is summarized in Figure 5-2.
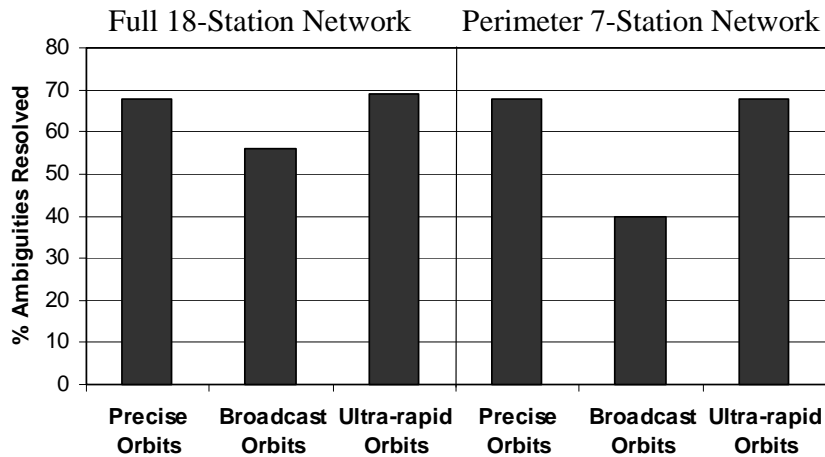
Figure 5-2. Ambiguity Resolution Capability Summary

Only the broadcast orbits introduced significant inability to resolve ambiguities. In the full network only 56 percent were able to be resolved, whereas in the degraded perimeter network only about 40 percent were consistently resolved. Also, both cases had circumstances where only 5 to 10 percent of the ambiguities were able to be resolved, indicating inconsistent and variant performance. However, precise and ultra-rapid orbits consistently showed little difference, with ambiguity resolution approaching the 70 percent mark regardless of the degradation case. The significant inability to resolve ambiguities using the broadcast orbits is a suspected contributor to the corresponding PW estimation errors. Quantification of the error contributions from each effect is unknown, as more focused examination would be required to do so.

Finally, the interpolation study showed some inadequacy for determining the PW distribution over the network region. Investigation up to this point demonstrated that the combination using near real-time ultra-rapid orbits and the degraded 7-station perimeter

network were the best combination to meet the constraints, having a minimal loss of PW estimation accuracy. However, this did not show the ability to characterize the precipitable water as it is distributed throughout the network region. With the 7-station perimeter network as a constraining factor, the only way to effectively determine the PW distribution is to use an interpolation or modeling method. Both a triangle-based linear and cubic interpolation schemes were employed to examine their performance in interpolating PW values throughout the network region. Both had marginal results, with consistent RMS errors greater than 5 millimeters at the most isolated (i.e., central) station locations. The cubic spline interpolation scheme showed slightly worse performance, but was chosen as the most likely characterization of the smooth distributions of PW.

A complimented network was considered where a centrally located station was included with the perimeter network. This was an attempt to minimally augment the data available, with hopes of significantly increased interpolation ability. However, RMS interpolation errors of more than 5 millimeters were still consistent in the most isolated regions of the network. Furthermore, overall improvement was rather sporadic with high dependence on the station location relative to the changing PW distributions. In the case of interpolating the precipitable water over the network, interpolated values are dependent upon both the distance from the neighboring data points and the distribution of the water vapor over the region. The combining effects of these factors render interpolation during varying weather conditions difficult to achieve. More subtle changes and uniform distributed vapor fields may be able to be interpolated effectively using the linear or cubic interpolation schemes, but more distributed and changing fields may take on the mask of more gradual changes. A better interpolation scheme or modeling

approach would be necessary to robustly characterize the precipitable water distribution over a network region.

5.3 Recommendations

Several areas for further analysis exist at each level of the GPS PW estimation process. First, and most basically, more precise coordinate estimation can be done in the initial setup phase. Fluctuations of several centimeters were assumed acceptable in this thesis, but may present a substantial error effect on the investigation into a small error component such as tropospheric delay. A longer period of observation data may be considered for accurately determining station coordinates within the network, prior to investigation into GPS PW determination. Also, the effects of coordinate accuracy on PW estimation could be independently quantified.

Secondly, further investigation of lower satellite elevation observations can be undertaken. This thesis used 10 degrees as a moderate cutoff level. However, lower elevations of 5 degrees or less may provide noticeable accuracy improvements in the estimation of zenith tropospheric delay and, ultimately, precipitable water. A tradeoff investigation of decreased satellite observation elevations versus the diminishing returns of increasing signal noise and corruption would be beneficial.

Moreover, this study used IGS ultra-rapid orbits that were produced at the beginning of each day under investigation. In essence, this should present the worst-case scenario where the error is maximized for this particular orbit case. The main restriction is that the IGS only produces ultra-rapid orbits twice daily, inhibiting regularly updating the orbit predictions. Improved PW estimation performance should result if an ultra-

rapid prediction was available at an hourly interval or less. This would require

development of a predicted orbit product of similar accuracy every interval period, or

using another data source such as the GAMIT formatted SCRIPPS orbit [10].

Additional efforts can be taken to quantify the separate effects of orbit accuracy

versus ambiguity resolution. It has been shown in this thesis that the combination of

these two effects significantly degrades PW estimation performance. Although most of

this poor PW estimation performance is suspected to be primarily associated with the

large orbit inaccuracies present in the broadcast ephemeris, the exact error contributions

of both remain uncertain.

A significant amount of research remains regarding interpolation or modeling

methods that may provide better water vapor field characterization over the network

region. Besides the basic triangle-based linear and cubic schemes evaluated in this thesis,

additional spline interpolation methods or least-squares collocation, amongst others, may

provide improved characterization ability. Application of different modeling methods

may also increase the ability to characterize the PW distribution over the network region.

Integrating meteorological models and profiles may be a valuable information source,

enhancing the ability to interpolate PW distribution over a network.

Another potential investigation involves the comparison of the different

processing software packages available in the use of precipitable water estimation.

Although each software package should inherently be very similar, small discrepancies

may render noticeably different PW results. This thesis showed effective PW

determination at station locations included in the network, but it may be possible to

further minimize the errors. Moreover, implementation of the mathematical PW

algorithm into a software package such as Bernese would also be a point of investigation. This may render more accurate results, as the process becomes a fluid process within the structure of the software itself.

On a broader scope, further investigation can be taken into the types of receivers and data that can be implemented into a network for GPS PW determination. In a military operating environment, military vehicles such as tanks, armored vehicles, and aircraft are dispersed throughout the region. These additional data sources could provide a valuable data augmentation to a GPS-MET network. In this case, the kinematic aspect of the receivers would need to be accounted for, as the vehicles are almost constantly in motion. Kinematic receivers would not be compatible with a surveying software package such as Bernese, requiring more advanced processing.

Finally, real-world implementation issues could be investigated. This would include many aspects including data storage, data retrieval, data transmission, automation, user interface, and other similar issues. Real-world implementation is typically one of the hardest areas to accomplish, due to the many inter-related issues involved.

Bibliography

[1]   Bevis, Michael, Steven Businger, Thomas A. Herring, Christian Rocken, Richard A. Anthes, and Rudolph H. Ware. "GPS Meterology: Remote Sensing of Atmospheric Water Vapor Using the Global Positioning System," *Journal of Geophysical Research*, Volume 97, No. D14, 15787-15801. 20 October 1992.

[2]   Bevis, Michael, Steven Businger, Steven Chiswell, Thomas A. Herring, Richard A. Anthes, Christian Rocken, and Rudolph H. Ware. "GPS Meterology: Mapping Zenith Wet Delays onto Precipitable Water," *Journal of Applied Meteorology*, Volume 33, 379-386. March 1994.

[3]   Businger, Steven, Steven R. Chiswell, Michael Bevis, Jingping Duan, Richard A. Anthes, Christian Rocken, Randolph H. Ware, Michael Exner, T. VanHove, and Frederick S. Solheim. "The Promise of GPS in Atmospheric Monitoring," *Bulletin of the American Meteorological Society*, Volume 77, No. 1, 5-18. January 1996.

[4]   Duan, Jingping, Michael Bevis, Peng Fang, Yehuda Bock, Steven Chiswell, Steven Businger, Christian Rocken, Frederick Solheim, Teresa Van Hove, Randolph Ware, Simon McClusky, Thomas A. Herring, and Robert W. King. "GPS Meteorology: Direct Estimation of the Absolute Value of Precipitable Water Vapor," *Journal of Applied Meteorology*, Volume 35, 830-838 (1996).

[5]   Hugentobler, U., S. Schaer, P. Fridez. *Bernese GPS Software Version 4.2*. Astronomical Institute: University of Berne, February 2001.

[6]   International GPS Service. Specifications of available data and products. http://igscb.jpl.nasa.gov/components/prods.html. n. pag. 22 May 2001.

[7]   The Mathworks, Inc., 21 Elliot Street, Natick, MA 01760. *MATLAB*®. 22 September 2000. Version 6.0. Release 12.

[8]   National Geodetic Survey Continuously Operating Reference Stations (CORS). Information and data for the CORS network. http://www.ngs.noaa.gov/CORS/cors-data.html. n. pag. 9 January 2002.

[9]   Nerem, R. Steve, David Whitlock. Real Time Atmospheric Water Vapor From GPS Using CORS and FSL Sites. Information and data for a research project. http://www.ae.utexas.edu/courses/ase389p_gps/projects99/whitlock/index.html. n. pag. 1 May 2001.

[10] NOAA Forecast Systems Laboratory Ground-Based GPS Meteorology Demonstration Network (GPS-MET). Information and data for the GPS-MET network. http://gpsmet.fsl.noaa.gov/jsp/index.jsp. n. pag. 27 July 2001.

[11] Raquet, John F. Class handout, ENG 533, Navigation Using The GPS. School of Engineering, Air Force Institute of Technology, Wright-Patterson AFB, OH. Spring 2001.

[12] Rocken, Christian, Teresa Van Hove, James Johnson, Fred Solheim, and Randolph Ware. "GPS/Storm—GPS Sensing of Atmospheric Water Vapor for Meteorology," *Journal of Atmospheric and Oceanic Technology*, Volume 12, 468-478 (1995).

[13] Ware, Randolph H., David W. Fulker, Seth A. Stein, David N. Anderson, Susan K. Avery, Richard D. Clark, Kelvin K. Droegemeier, Joachim P. Kuettner, J. Bernard Minster, and Soroosh Sorooshian. "SuomiNet: A Real-Time National GPS Network for Atmospheric Research and Education," Unpublished, to appear in: *Bulletin of the American Meteorological Society*, April 2000.

[14] Zhang, JiHong. *Investigations into the Estimation of Residual Tropospheric Delays in a GPS Network.* MS Thesis. University of Calgary, Calgary, Alberta, Canada, November 1999 (UCGE Reports Number 20132).

Vita

2nd Lieutenant David A. Garay grew up in Milwaukee, Wisconsin where he graduated from Milwaukee Trade and Technical High School in June 1996. He went on to obtain a Congressional Appointment to the United States Air Force Academy near Colorado Springs, Colorado, where he earned his Bachelor of Science Degree in Electrical Engineering in May 2000.

Having been appointed a Second Lieutenant in the United States Air Force in 2000, his first assignment was to the Air Force Institute of Technology at Wright-Patterson AFB, OH. 2Lt Lieutenant David A. Garay will graduate with his Masters Degree in Electrical Engineering with a focus on Guidance, Navigation, and Control in March 2002. His assignment, following AFIT completion, is to the 746th Test Squadron at Holloman AFB, NM where he will be field-testing advanced GPS, INS, and other avionics technologies.

REPORT DOCUMENTATION PAGE

1. REPORT DATE *(DD-MM-YYYY)*	2. REPORT TYPE	3. DATES COVERED *(From – To)*
15-03-2002	Master's Thesis	Aug 2000 – Mar 2002

4. TITLE AND SUBTITLE	5a. CONTRACT NUMBER
ESTIMATION OF ATMOSPHERIC PRECIPITABLE WATER USING THE GLOBAL POSITIONING SYSTEM	5b. GRANT NUMBER
	5c. PROGRAM ELEMENT NUMBER
6. AUTHOR(S)	5d. PROJECT NUMBER
Garay, David A., 2Lt, USAF	5e. TASK NUMBER
	5f. WORK UNIT NUMBER

7. PERFORMING ORGANIZATION NAMES(S) AND ADDRESS(S)	8. PERFORMING ORGANIZATION REPORT NUMBER
Air Force Institute of Technology Graduate School of Engineering and Management (AFIT/EN) 2950 P Street, Bldg 640 Wright-Patterson AFB OH 45433-7542	AFIT/GE/ENG/02M-07

9. SPONSORING/MONITORING AGENCY NAME(S) AND ADDRESS(ES)	10. SPONSOR/MONITOR'S ACRONYM(S)
Air Force Weather Agency (AFWA) Technical Transition Team Attn: Captain Robert T. Swenson, Jr. 106 Peacekeeper Drive, Suite 2N3 Offutt AFB, NE 68113-4039 DSN 271-1672 COMM (402) 294-1672	AFWA/DNXT
	11. SPONSOR/MONITOR'S REPORT NUMBER(S) N/A

12. DISTRIBUTION/AVAILABILITY STATEMENT
APPROVED FOR PUBLIC RELEASE, DISTRIBUTION UNLIMITED.

13. SUPPLEMENTARY NOTES

14. ABSTRACT

This thesis focuses on using the Global Positioning System (GPS) for atmospheric precipitable water (PW) estimation. Water vapor, measured in terms of PW, plays a crucial role in atmospheric processes and short-term weather forecasting. Traditional methodologies for measuring atmospheric water vapor distributions have known inadequacies, resulting in the motivation to gain good water vapor characterization via GPS. The ability to accurately forecast cloud formation and other weather phenomenon is critical, especially in the case of military operations.

Using a network of GPS receivers, it is possible to estimate precipitable water throughout the network region with better accuracy than traditional methods and on a more consistent near real-time basis. First, an investigation into the effects of introducing less accurate, near real-time GPS ephemerides was accomplished. Secondly, the network geometry and data availability were degraded to simulate potential military operational constraints. Finally, several interpolation methods were applied to quantify the ability to estimate the water vapor distribution over the entire network region with limited data availability and network geometry constraints.

Results showed that International GPS Service (IGS) ultra-rapid orbits introduced minimal PW estimation error (~1-2 mm) while maintaining near real-time capability. The degraded perimeter network also introduced minimal PW estimation error (~1-2 mm) at the included stations, indicating potential application in constrained data environments. However, the interpolation investigation showed an overall inability to determine PW distribution over the entire network region.

15. SUBJECT TERMS
Global Positioning System, GPS, Differential Global Positioning System, DGPS, GPS Meteorology, GPS-MET, Precipitable Water, Atmospheric Water Vapor

16. SECURITY CLASSIFICATION OF:			17. LIMITATION OF ABSTRACT	18. NUMBER OF PAGES	19a. NAME OF RESPONSIBLE PERSON
a. REPORT	**b. ABSTRACT**	**c. THIS PAGE**			Raquet, John F., Major, USAF
U	U	U	U	119	**19b. TELEPHONE NUMBER** *(Include area code)* 937-255-3636 x4580